# Earths-Field-NMR Remote

**Physikalisches Fortgeschrittenenpraktikum at University of Constance**

Authors: Philipp Gebauer, Simon Keegan and Marc Neumann

Tutors: Narinder Narinder and Matthias Falk

Execution on 9th and 27th of July 2020

## Abstract

The aim of this report is to show the principals of an EFNMR measurement and to discuss its results.
The first part of the experiment is about the basic principal of an EFNMR measurement. Therefore the noise level is taken into account and is identified to be 7.5 $\mu$V for our setup. In order to tune the circuit to the lamor frequency of hydrogen at 1841.4 Hz, the LCR circuit in the $B_1$ coil has to have a capacity of 13.8 nF. To obtain a sharp peak in the spectrum of the measured hydrogen signal the system was tuned to following values: shimming values $x = 10.11\,\mathrm{mA}$, $y = 20.88\,\mathrm{mA}$, $z = -20.07\,\mathrm{mA}$; $B_1$ pulse duration 1.35 ms; capacity 13.8 nF. The relaxation time measurements in the polarizing field results in values for $T_{1,p}$ of 2912.8800(48) ms. The relaxation time measurements in the earths magnetic field results in values for $T_{1,e}$ of 2753.0500(12) ms. The measurements of $T_2$ results in values of 2691(12) ms with single *Hahn* echos and 2317.760 00(62) ms with the use of 30 echos in a CPMG.
hier noch was zum zweiten teil schreiben!

All authors have worked equally on all parts of this report and used no other sources than listed in the bibliography.

# Contents

# 1 Introduction

Earths field nuclear magnetic resonance is a widely used method in the quality management or in medical technology to gain knowledge about the structure of materials. Therefore the magnetic moment of spins is taken into account.
Due to the external magnetic field of the earth $B_0$ (sometimes refered to as $B_e$) the spins of hydrogen (spin quantum number: $I = \frac{1}{2}$) align either parallel or antiparallel to this magnetic field. Using the BOLTZMANN statistics it can be calculated, whether the spins are aligned parallel or antiparallel. Therefore the information about the temperature and the surrounding magnetic field $B_0$ is necessary. Each spin precesses around the surrounding magnetic field $B_0$ (along z-axis), most of the time in the spin up direction because it is energetically more favorable. This precession evokes a component of the spins in the transversal plane. However, since the phase of the precession is random the net magentization is aligned along the z-axis. By changing the properties of the surrounding magnetic field, the bulk magnetization vector can be manipulated. In order to do so an alternating electro magnetic field pulse is applied. The frequency of this magnetic field ($B_1$) is in the radio frequency (RF) magnitude for large $B_0$ and for low $B_0$ it is in the ultra low frequency (ULF). Since we use the earths magnetic field $B_e$ for our measurements, the frequency is in the ULF magnitude. When the frequency of this magnetic field pulse is chosen right at the larmor frequency of the sample, the transitions between the energy levels of spin up and down are more likely to happen and therefore a phase coherence of the spins occurs. The applied pulse results in changing the spins direction by a tipping angle $\Theta$ from the vertical to the transversal plane. The precession of the spins can be measured in the transversal plane by a coil ($B_1$ coil) which is aligned orthogonal to the earths magnetic field. The $B_1$ coil is therefore the exciting and detecting coil and therefore the heart of our measurements.
The first part of this experiment is about the basics of ENMR. At first we have a look at the noise that is dependent on surrounding metal objects. Then we analyse the $B_1$ coil by changing the capacity of the LCR circuit. The next step is the optimization and characterization of a free induction decay (FID) of a water sample. The aim of this chapter is to measure a sharp peak at the larmor frequency of the hydrogen in the water. When this is done the longitudinal relaxation time $T_1$ and the transversal relaxation time $T_2$ are measured and discussed. hier noch was zum zweiten teil schreiben!

# 2 Setup

This chapter is about the setup of this experiment. To understand which part of the experiment has what use, it is necessary to have a look at the components of the setup. Figure 2.1 shows the different coils which are necessary for the EFNMR measurement. The inner coil $B_1$ is the excitation and collection coil which is described in the previous chapter. The outer coil is used to prepolarize the sample. This is necessary to obtain a strong signal. By applying a strong magnetic field, all spins align in the direction of the prepolarising pulse and provide a bulk polarised nuclear magnetization across the sample. The middle coil is called the gradient coil. This coil erases the inhomogeneous magnetic field which always occurs for different uncertainty reasons. This coil is also used for the 2D imaging of the probe by adjusting the components of the magnetic field.
The z-axis of the whole setup of coils has to be aligned parallel to the earths magnetic field. Therefore a compass can be used to adjust the position. Via the computer program *Prospa* and the spectrometer, the currents of the coil can be adjusted and the induced signals can be measured.

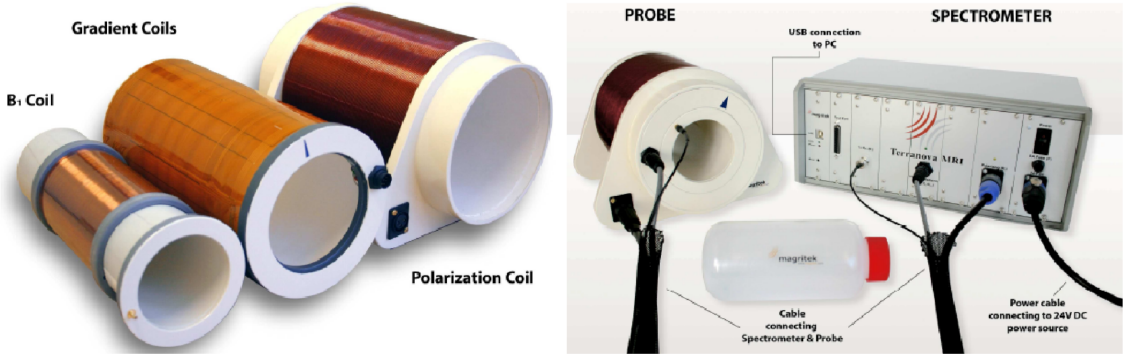


**Figure 2.1:** Setup of the *Terranova-MRI EFNMR*. On the left-hand side the coils $B_1$ (excitation and collection coil), gradient coil (homogeneous magnetic field and 2D scanning coil) and the prepolarising coil $B_p$ are displayed. The right-hand side shows the water sample which has been used and the spectrometer which adjusts the necessary signals to the coils. [Mor01]

# 3 Part I – Basics

## 3.1 Noise measurement

The first step in the EFNMR Remote experiment is to measure the external noise. The external noise depends on the location where the setup is placed, the orientation of the probe and on surrounding metal objects e.g. a metal desk. To detect this external noise, a measurement without an NMR signal is provided. The time domain noise signal is shown in figure 3.1. It is clearly visible that the noise is centered around 0 $\mu$V. To gain knowledge about the noise level, the computer calculates the root-mean-square (RMS). This means that it calculates the square of each data point, then sums up all the squared values, calculates the average and then applies a square root. With this method the noise level can be calculated. In this case it has a value of 7.5 $\mu$V. This is of an acceptable magnitude because any value below 10 $\mu$V is good enough to provide meaningful NMR data.

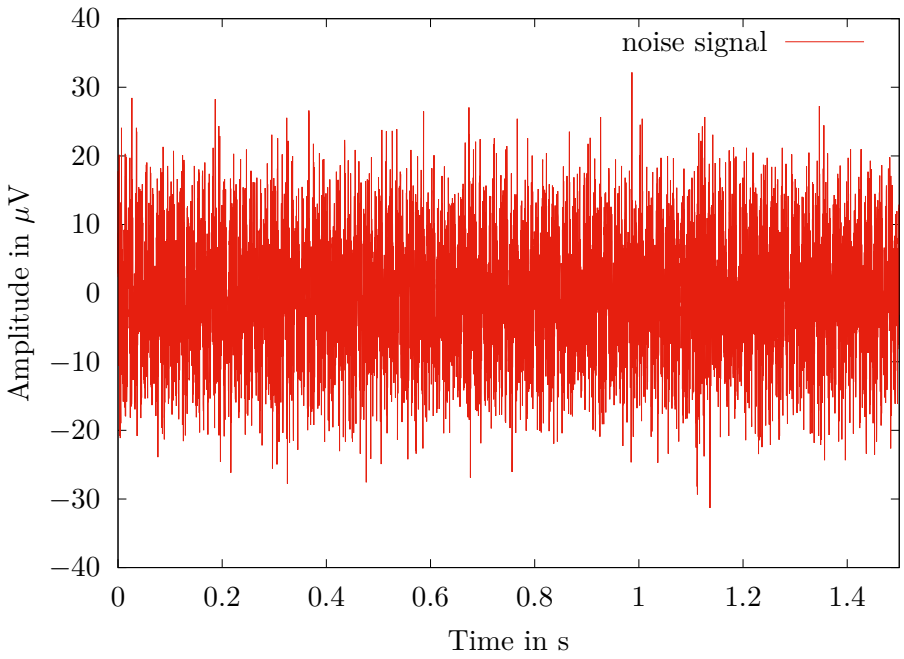


**Figure 3.1:** Noise signal taken by the $B_1$ coil. The noise value of this signal is 7.5 $\mu$V.

Figure 3.2 shows the frequency domain noise. This means that the time domain is fourier transformed into the frequency domain. This method is one of the basic principles used in this experiment to make research about the properties of the measured signals. The frequency domain noise shows very specific sharp peaks every 50 Hz interval. To be more

precise the peaks in the middle of every hundred Hz step are way higher than those at 1400 Hz, 1500 Hz and so on. This results from the frequency in the power grid which is 50 Hz in Germany and can also be affiliated to the electrical noise of a surrounding fluorescent light or the CRT computer monitor. Unfortunately the remote camera program of the computer did not work and therefore it is not clear if there was a fluorescent light in the room. Even though the noise peaks in the frequency domain figure 3.2 indicate that there could be a fluorescent light source in the room. Despite all sharp peaks, there is also a slight increase of the amplitude around $185(10) \cdot 10^1 \frac{\mu V}{Hz}$ visible. This is explicable by the resonance frequency of the instrument and its sensitvity around the larmor frequency (1841.4 Hz for water in Germany in July 2020). All our following measurements will be done nearby the larmor frequency. That is the reason why the instrument sensitvity is sharpend around this value.

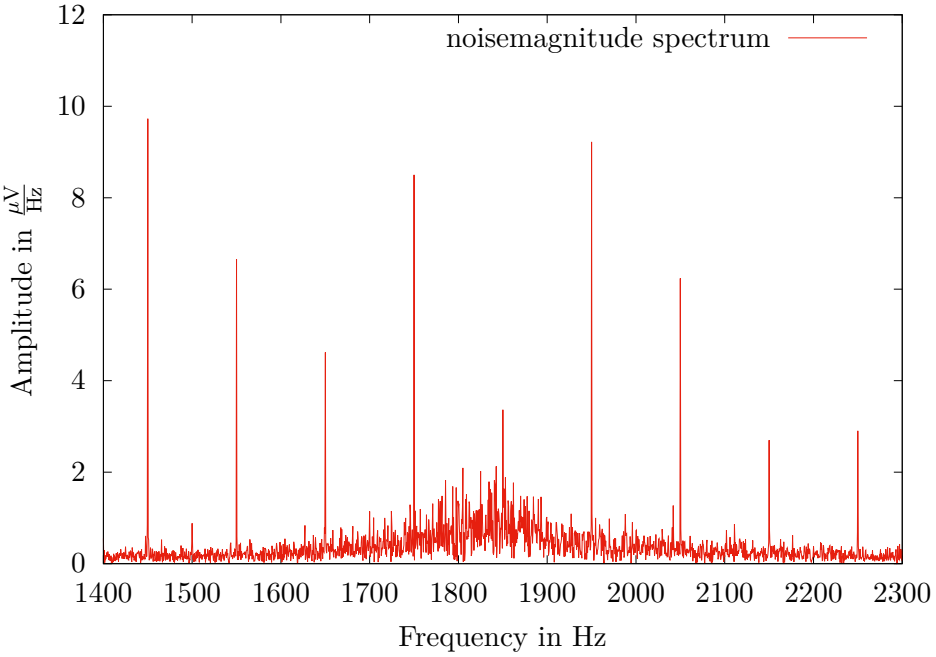


**Figure 3.2:** Fourier transformed noise signal of the previous figure 3.1. Strong peaks every 50 Hz correspond to the frequency of the power grid in Germany and to electrical noise of a surrounding fluorescent light or the CRT computer monitor. The slight increase of the amplitude around $185(10) \cdot 10^1 \frac{\mu V}{Hz}$ is explicable by the resonance frequency of instrument and its sensitvity around the larmor frequency (1841.4 Hz for water in Germany in July 2020).

## 3.2 Coil Analysis

Now knowing that we have an acceptable noise value of less than $10\,\mu$V, we can analyse the coil. In order to do so we explain the general approach of NMR signals first. To measure a NMR signal a pulse and collect measurement has to be done. Therefore the $B_1$ coil (transmit and collect coil) has to apply a pulse. This pulse changes the spins direction out of its thermal equilibrium (along z-axes, due to the earths magnetic field $B_e$) into a direction with a component in the transversal plain. Therefore the $B_1$ coil collects a signal because it is aligned orthogonal to $B_e$. The transmit and collect procedure is based on FARADAY's law of induction. Figure 3.3 exemplary shows such a pulse and collect signal by the $B_1$ coil. Every following measurement in this report is based on the procedure of pulse and collect.

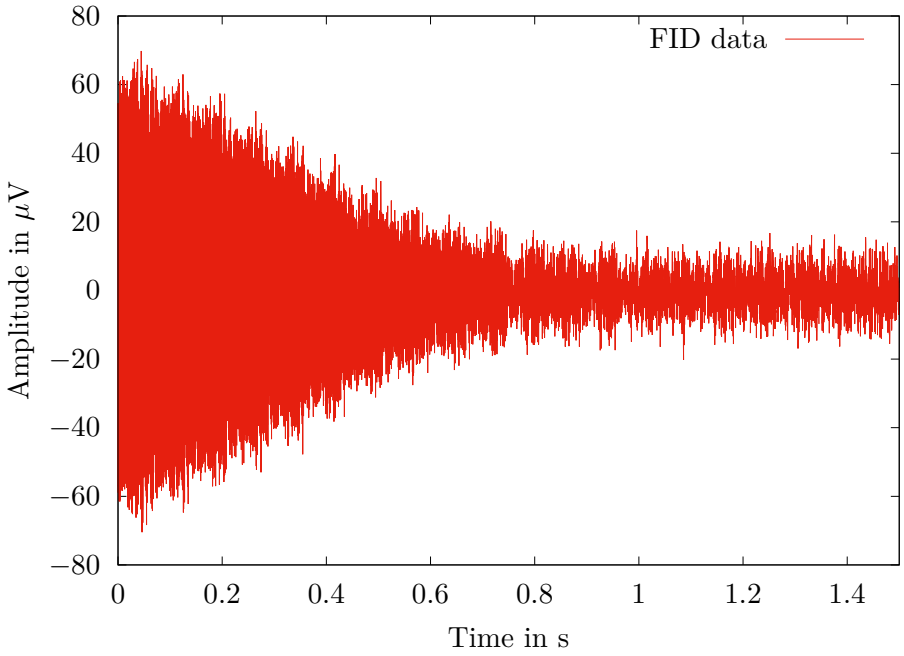


**Figure 3.3:** Example signal for a pulse and collect signal made by the $B_1$ coil. The example signal is taken from a FID signal.

Due to the fact that the $B_1$ coil is a tuned LCR circuit a resonance frequency exists, which can be calculated by the following formula:

$$\omega_{calc} = \frac{1}{\sqrt{L \cdot C}} \,. \tag{3.1}$$

In order to analyse the $B_1$ coil the resonance frequency, depending on the capacity, is

measured. Therefore the $B_1$ coil transmits a signal. Due to this signal the response of the coil can be measured. This signal is then fourier transformed and the resonance frequency can be deduced from the frequency domain (maximum in the frequency domain). This procedure is repeated automatically by the computer programm *Prospa* for different capacities. By changing the capacity we can examine the best capacity in dependence of the larmor frequency. Figure 3.4 shows the measured and theoretically calculated resonance frequency (equation (3.1); $L = 0.417\,\mathrm{H}$) in dependence of the capacity. The horizontal line represents the larmor frequency of 1841.4 Hz for hydrogen in Germany in July 2020. To gain this value the vertical component of the earths magnetic field (43 248.8 nT [Adm]) is multiplied by the gyromagnetic ratio $42.577\,\frac{\mathrm{MHz}}{\mathrm{T}}$ [Adm]. The vertical line represents the correct capacity we should use for our measurement, due to the resonance frequency of the larmor frequency. In this case the correct capacity is 13.8 nF. Corresponding to the calculated resonance frequency the correct capacity would be 17.9 nF. It is not deniable that the measured curve is not parallel to the measured resonance frequency. This probably has its cause in the not fixed inductance $L$. Due to heating of the coil $L$ might change a little by increasing capacity and thus the calculated curve does not fit to the measured one. Another reason for the different calculated curve is that we used real coils and those have parasite resistances and also built-in capacities. This built-in capacity is not taken into account in the formula (3.1) and therefore the calculated curve might be not correct. Since the calculated curve does not fit to the measured one, the calculated value for the capacity is not taken into account.

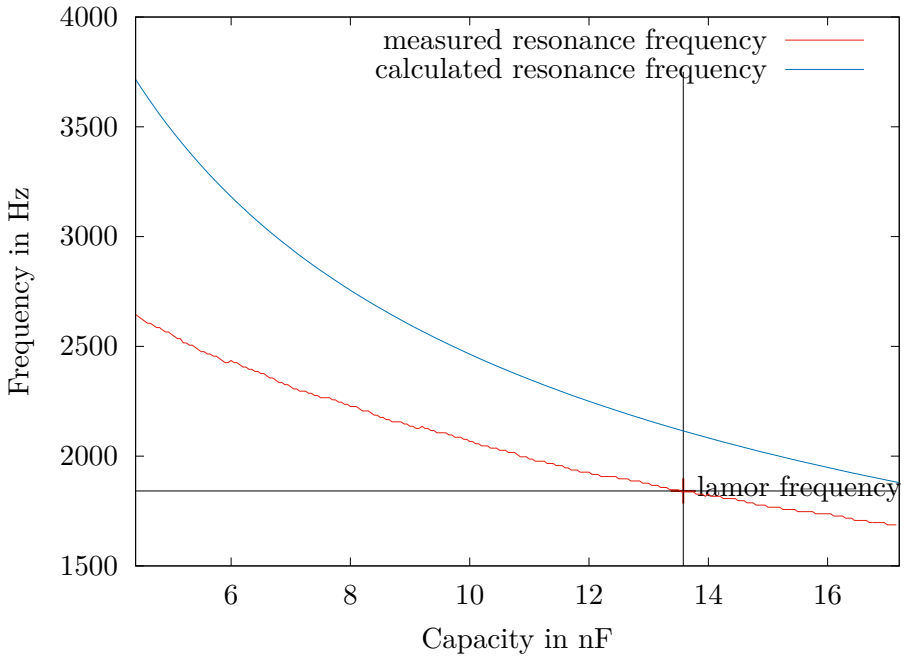


**Figure 3.4:** This figure shows the measured and calculated resonance frequencies for different capacities. The marked cross represents the larmor frequency of 1841.4 Hz for hydrogen in Germany in July 2020.

## 3.3 Optimization and Characterisation of FID in water sample

One of the main goals of this experiment is to measure a good FID of the water sample. In order to do so we first have to optimize our FID signal of the water probe.
At first the inhomogeneity of the magnetic field has to be cancelled. The process to make the magnetic field more homogeneous is to *autoshim* the components of the gradient coil. The computer program does this automatically. So it de-shims the system step by step and checks if the output maximizes or minimizes. By checking many different combinations it finds the best shimming values for the gradient coil. In our case they are:

$$x = 10.11\,\mathrm{mA}$$
$$y = 20.88\,\mathrm{mA}$$
$$z = -20.07\,\mathrm{mA}\ .$$

That means with those shimming values the magnetic field in the setup is as homogeneous as possible.
The second optimization step is to change the $B_1$ pulse duration. The longer the pulse

duration is, the larger is the angle of the flipping spins and thus the signal will get stronger (only for flipping angles up to 90°). The best signal is obtained for a flipping angle of 90° because with this angle the spins only have a component in the transversal plane and therefore the signal is maximized. If the pulse duration is too long, then the flipping angle is larger than 90° and the spins get a horizontal component again and the signal will decrease again. When a flipping angle of 180° is reached the signal will be at its minimum. Afterwards the signal will rise again because of the increasing horizontal component. Figure 3.5 shows this issue. The maxmimum at a pulse duration of 1.35 ms is clearly visible. This means that after applying a $B_1$ pulse with a duration of 1.35 ms the spins are in the transversal plane and therefore the best signal is obtained.

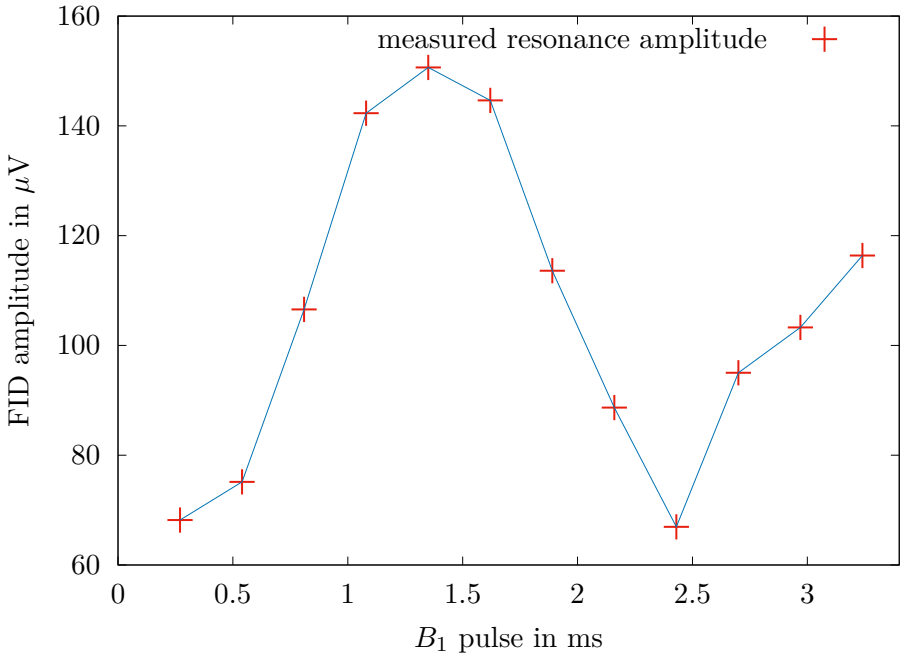


**Figure 3.5:** This figure shows which impact the $B_1$ pulse duration has on the amplitude of the FID. It is clearly visible that the duration has a maximum at 1.35 ms which is the duration for a 90° pulse.

Figure 3.6 exemplary shows the correlation of the $B_1$ pulse duration and the signal which the coil detects. It is clearly visible that the amplitude is higher for a pulse duration of 1.35 ms than for a pulse duration of 0.27 ms. The signal that was taken for the pulse duration of 0.27 ms is at the minimum of the figure 3.5 and therefore it is correct that the amplitude of the spectrum with the pulse duration of 1.35 ms is higher.

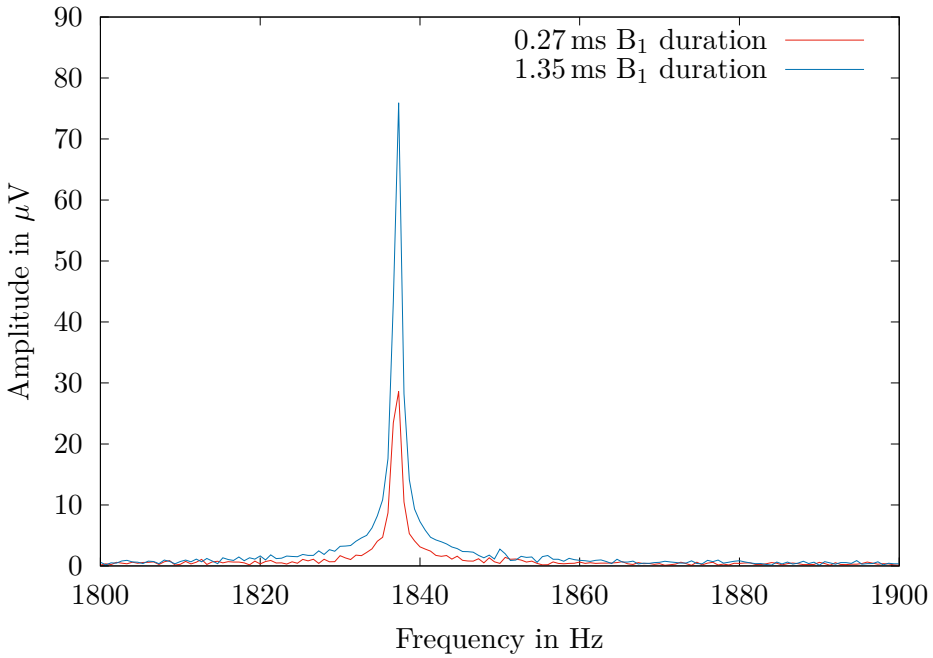


**Figure 3.6:** Example spectrum for two different $B_1$ pulse durations. The peak which is higher corresponds to the 1.35 ms duration pulse and represents the 90° pulse. This peak is high because at this duration most of the spins are in the transversal plane and therfore the amplitude is at its maximum.

Now that the $B_1$ pulse duration is also optimized, we can have a closer look at the capacity of the LCR circuit of the $B_1$ coil again. First it is necessary to know that the $B_1$ pulse is applied by a *rectangular* function and the fourier transform of a *rectangular* function is a *sinc* function. Therefore the fourier transformed spectrum of the $B_1$ pulse signal is a *sinc* function. When we measure the signal shortly (acquisition delay: 2 ms) after the 90° pulse, there should be a *sinc* function visible and indeed this is what we obtained (figure 3.7). In figure 3.7 there is also a really sharp peak visible. This is referred to the hydrogen signal. The hydrogen signal is independent of the applied capacity, but the $B_1$ pulse is, because the capacity changes the properties of the LCR-circuit, of the $B_1$ coil. The best capacity is adjusted when the hydrogen signal is located in the middle of the *sinc* function because then the LCR-circuit is tuned to the larmor frequency of the hydrogen signal. This is also visible by the amplitude of the spectrum in figure 3.7. The amplitude of the spectrum which was observed for a capacity of 13.8 nF is higher than for the amplitude of the spectrum which was observed for a capacity of 14.2 nF. As already explained before in chapter 3.2 the capacity of 13.8 nF is indeed the best capacity in order to observe a maximized spectrum.

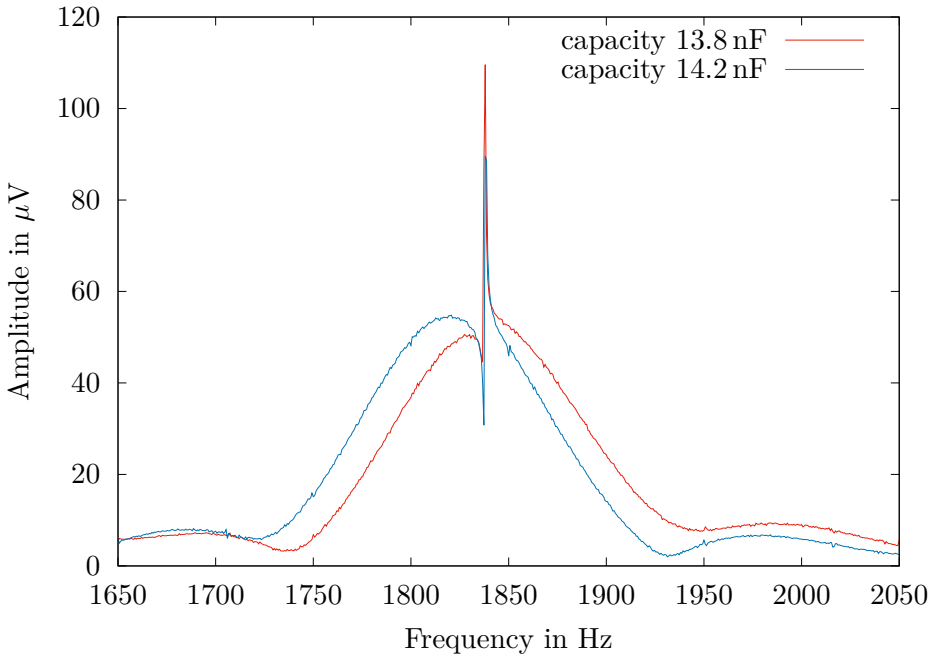


**Figure 3.7:** This figure shows the impact of the capacity in the LCR circuit of the $B_1$ coil. The *sinc* function comes from the fourier transformed $B_1$ pulse, which is rectangular. The peak at 1837.27(5) Hz is due to the the hydrogen signal.

Now that the FID signal is optimized best we can start to characterize it. Therefore we measure a FID with a acquisition delay of 25 ms because after this delay there are no effects from the rectangular applied $B_1$ pulse anymore (no *sinc* function in the spectrum). Figure 3.8 shows the observed spectrum and two different fit possibilities.
One option to fit a peak in a spectrum is by applying a VOIGT profile ($V(x;\sigma,\gamma)$). This function is a convolution of the CAUCHY-LORENTZ and GAUSSIANdistribution and is described by the following formula:

$$V(x;\sigma,\gamma) = (G \star L)(x) = \int G(\tau)L(x-\tau)d\tau \tag{3.2}$$

$$G(x;\sigma) = \frac{\exp\left(\frac{-x^2}{2\sigma^2}\right)}{\sigma\sqrt{2\pi}} \tag{3.3}$$

$$L(x;\gamma) = \frac{\gamma}{\pi\left(x^2+\gamma^2\right)} \ . \tag{3.4}$$

The standard deviation is represented by $\sigma$, $\gamma$ specifies the half of the peak width at half height from the LORENTZ distribution and $x$ is the shift from the line center. In figure 3.8 the VOIGT profile (green) is fitted to the measured spectrum (red). The problem

of this fit is that it is not as sharp as the measured data. This might be due to the fact that the measured spectrum does not have many data points especially around the maximum. Therefore the peak is really sharp and a correct fit with the VOIGT profile is rather difficult. Therefore a second fit function has been applied. This time only the GAUSSIAN distribution was used. This fit function is better to calculate the width of the peak, due to the fact that it is easier to fit it to this narrow peak. The full width of the peak at half maximum (FWHM) is calculated by the applied GAUSSIAN fit and is quantified as 1.177(42) Hz.
The amplitude of the peak is 73.85 $\mu$V according to the GAUSSIAN fit and is in comparison to the amplitude of the noise measurement (magnitude 1) in figure 3.2 rather high. The signal to noise ratio at this point is 47.57. To calculate this value the amplitude at 1837.27 Hz (center of the peak) in figure 3.8 is devided by the value of the amplitude at the same frequency in figure 3.2. That value clearly shows that the peak must arise from the hydrogen signal and is barely disturbed by any noise.
The width of the measured hydrogen peak at half height (FWHM) is 1.177(42) Hz and hence really sharp. An even better value can only be achieved by tuning the setup even more. To show the physical properties, this value is though of a really good size.
The disadvantage of the GAUSSIAN fit is that the area under the curve does not equal the measured one, especially around 1836 Hz and 1839 Hz. Therefore the discussion of the integral under the measured curve will just be qualitative and will be done in chapter 3.5.
It is also possible to take a measurement of the imaginary signal of the peak in figure 3.8. Unfortunately we did not safe this data. Beacuse of that we explain what we should see and what it means. The imaginary component describes the dispersion spectrum. The spectrum then has to look like a hyperbolic function with the pole exactly at 1837.27 Hz (center of the peak). Since it is no real hyperbolic function there exist values at the pole. Those values are aligned in a vertical line.

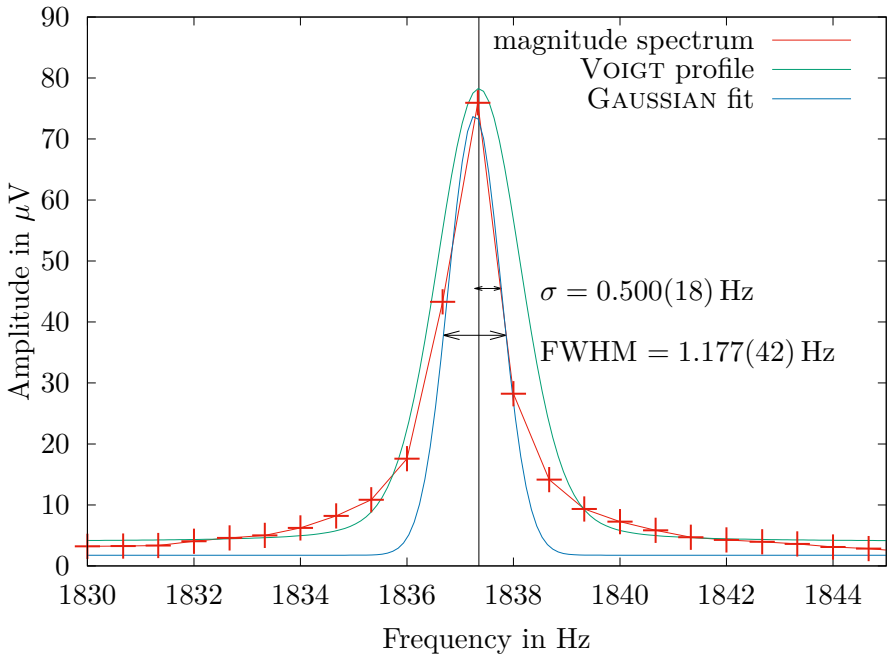


**Figure 3.8:** This figure shows the measured hydrogen signal after an acquisition delay of 25 ms and two possible ways to fit the peak. Due to a very short frequency range the peak looks very wide. Indeed it is actually very sharp. To fit the peak a VOIGT profile and GAUSSIAN fit is used.

## 3.4 Longitudinal relaxation measurements T1

There exist two possibilities to measure the longitudinal spin lattice relaxation. First we want to have a closer look at the measurement via $\tau_p$ (polarizing pulse duration). Therefore the computer program *Prospa* applies a polarizing pulse orthogonal to the earths magnetic field. Due to this polarizing pulse the spins align in the transversal plain and form a bulk magnetization. By time the magnetization becomes stronger because of this the signal becomes stronger. This relation is visualized in the figure 3.9.

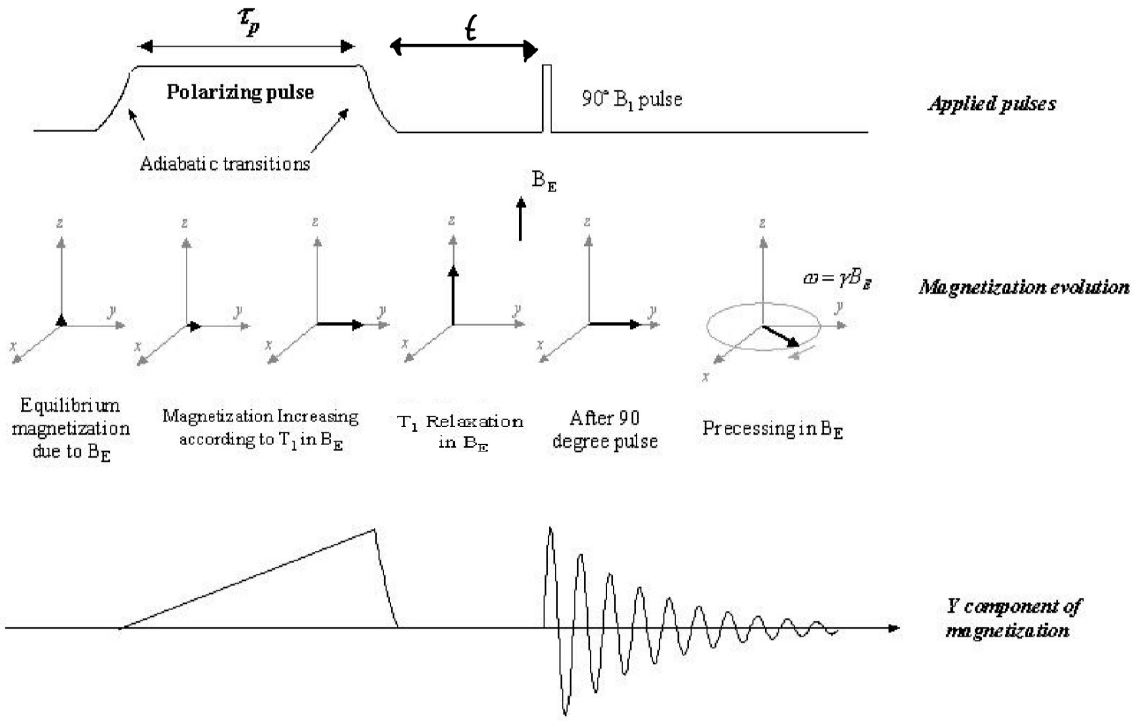


**Figure 3.9:** Sketch to show how $T_1$ can be measured. One way is by changing the polarizing pulse duration $\tau_p$ and the other way is by varying the time between the polarizing pulse and the 90° pulse. [Mor01]

Due to the increasing magnetization it is possible to calculate the $T_{1,p}$ relaxation. In order to do so the magnetization time is increased step by step from 500 ms to 4500 ms with an increment of 500 ms and in each configuration the signals maximum is obtained from the fourier transformed spectrum. Figure 3.10 shows the attenuation of the signals normalized to the maximum peak $E_0$. The underlying idea is that by applying a fit function as following:

$$S(x) = S_0 \cdot \left[1 - \exp\left(\frac{-x}{T_{1,p}}\right)\right] \ , \tag{3.5}$$

it is possible to calculate the relaxation time $T_{1,p}$. The exponential decay is a result of the loss of phase coherence between the spins and will be used for every measurement of spin relaxation. In this case $T_{1,p}$ is found to count as 2912.8800(48) ms.

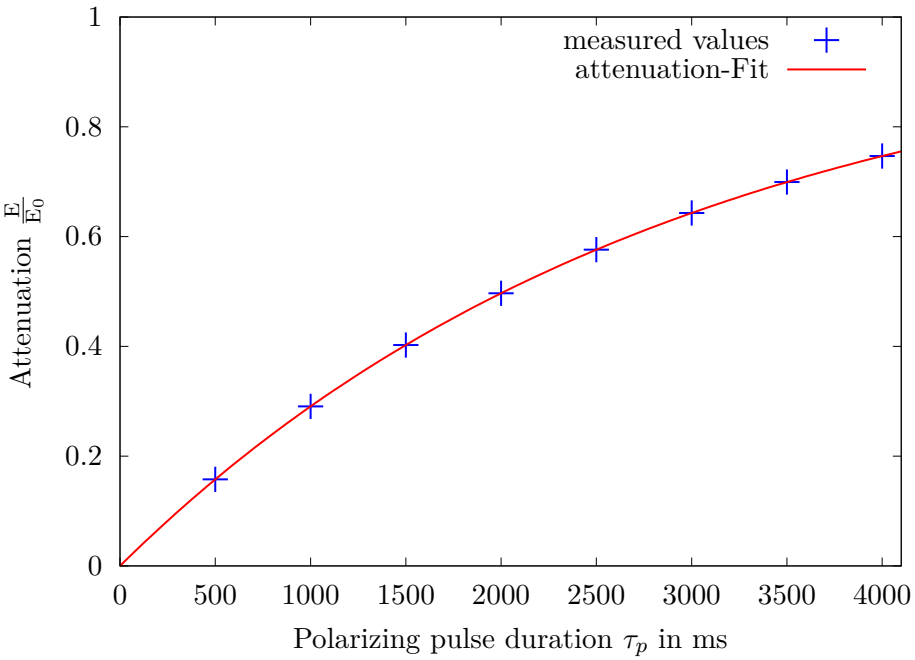


**Figure 3.10:** $T_{1,p}$ measurement by varying $\tau_p$ and observing how the attenuation $\frac{E}{E_0}$ evolves. The provided exponential fit results in a value for $T_{1,p}$ of 2912.8800(48) ms.

The second option is to calculate the spin lattice relaxation via the earths magnetic field $B_e$. In this case the index will be chosen as "$e$" for the spin lattice relaxation. The procedure in this case is to change the time $t$ (pre-90 minimum delay) between the polarizing pulse ends and the 90° pulse begins. This relation is also visualized in figure 3.9. The pre-90 minimum delay is chosen as 0 ms and the pre-90 delay step size as 500 ms. For every configuration the signal maximum is calculated again of the fourier transformed spectrum. Figure 3.11 shows the attenuation of the signals normalized to the maximum peak $E_0$. This time the $T_{1,e}$ can be calculated by the following fit function:

$$S(x) = S_0 \cdot \exp\left(\frac{-x}{T_{1,e}}\right) \quad . \tag{3.6}$$

In our case $T_{1,e}$ is observed to be 2753.0500(12) ms.
In both ways the uncertainty of the $T_1$ values are quite small. This is the result of really good aligned values to the fit function. Nevertheless $T_{1,p}$ and $T_{1,e}$ are not consistent even though the uncertainty is considered. This might be, due to the fact that those two measurements are based on two different methods and $T_{1,e}$ is dependent on the earths

magnetic field. Even though they are not consistent, the values for $T_{1,p}$ and $T_{1,e}$ have the same magnitude and also have the same magnitude according to a literature value of 4000 ms [LLC]. It is good to keep in mind that a comparison to literature values is just there to get the magnitude. Since the surrounding magnetic field and the probe define the exact value.

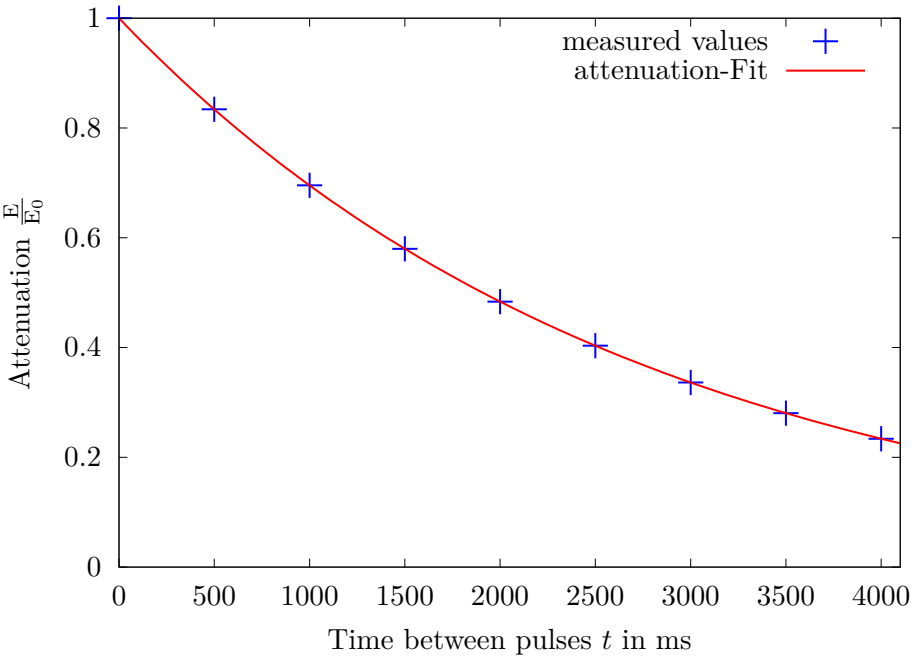


**Figure 3.11:** $T_{1,e}$ measurement by varying $t$ and observing how the attenuation $\frac{E}{E_0}$ evolves. The provided exponential fit results in a value for $T_{1,e}$ of 2753.0500(12) ms.

## 3.5 Hahn echo

Another relaxation measurement considers the time $T_2$, also referred to as the transversal relaxation time. In order to understand that, we first have to explain the HAHN echo and the principle of multiple echo sequences.

The principle of the HAHN echo is that an 90° pulse is applied and after a certain time $\tau$ a 180° pulse. The reason behind this method is, that after the 90° pulse was applied the spins are oriented in the transversal plane and start to precess around the earths magnetic field vector (z-axis). Due to spin-spin interaction (inhomogeneous magnetic field accrues) the spins also interact with each other and therefore some spins have a higher larmor frequency and some have a lower one. If an 180° pulse is applied after a certain time the

spins will flip in the transversal plane and the slow precessing spins will be located before the fast precessing spins again and when the fast precessing overtake the slow ones the $B_1$ coil will detect a signal again. The reason why the $B_1$ coil does not detect a signal while the slow and fast precessing spins are at different positions is that they erase each other, considering them as a superposition. If the spin-spin interaction is too weak then it also helps to de-shim the system along the x-direction. This also makes the homogeneous magnetic field inhomogeneous and thus the spins will get different larmor frequencies according to their position.
Figure 3.12 exemplary shows the HAHN echo for a shimming value of 4.95 mA along the x-axis (original value 10.11 mA). It is also possible to change the time between the 90° and 180° pulse. This would shift the peak to higher values in the timescale and due to loss effects, the amplitude would shrink a little bit.

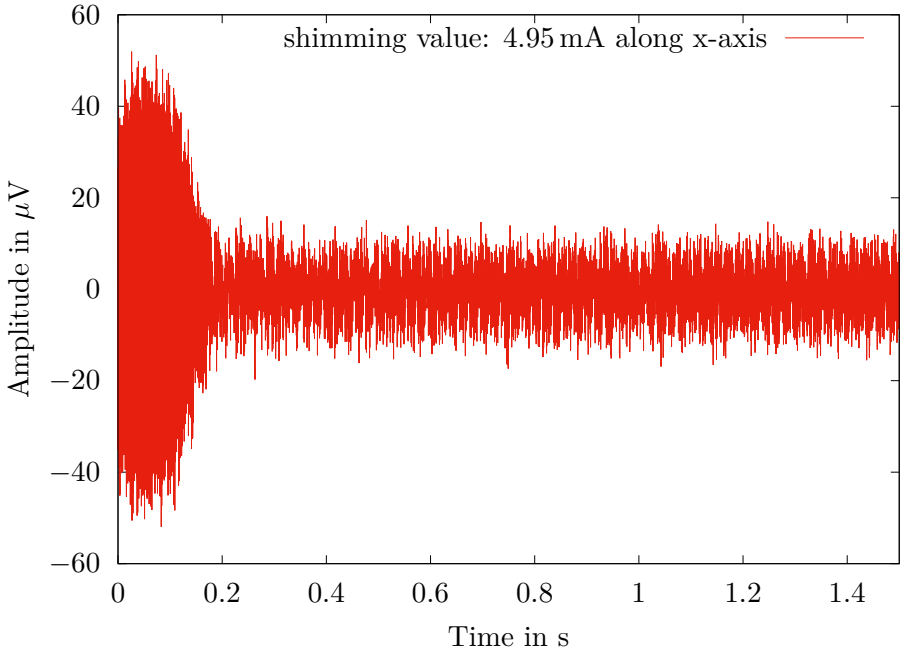


**Figure 3.12:** Example measurement of a single HAHN echo for an echo time of 0 ms. The maximum of the echo is clearly visible. Due to relaxation after the maximum the detected signal at times after about 0.2 s is noise.

It is also possible to fourier transform the signal from figure 3.12. This is shown in figure 3.13 for two different shimming values. The amplitude of the spectrum with the shimming value of 0 mA along the x-axis is unambiguously smaller than the amplitude of the spectrum with shimming value of 4.95 mA along the x-axis. This effect is a result of

the more inhomogeneous magnetic field of the spectrum with the shimming value of 0 mA along the x-axis. A more inhomogeneous magnetic field also has the consequence that the spins have more different larmor frequencies and thus the total intensity shrinks. The area beneath the graph should be independent of the inhomogeneity because in total the magnetization has to be the same. Only the distribution is different. This effect is also clearly visible in figure 3.13. This time it is not possible to find a good fitting function. Therefore this discussion is more qualitative as mentioned before in chapter 3.3. The reason why there is no good fitting function is that there are a lot of randomly occurring peaks in the spectrum and the more peaks there are the more difficult it is to find a good fitting function. Another thing that makes it rather hard is that the frequency steps are not quite small and thus there are few datapoints to make a good fit. This also was a problem in chapter 3.3 as mentioned before.

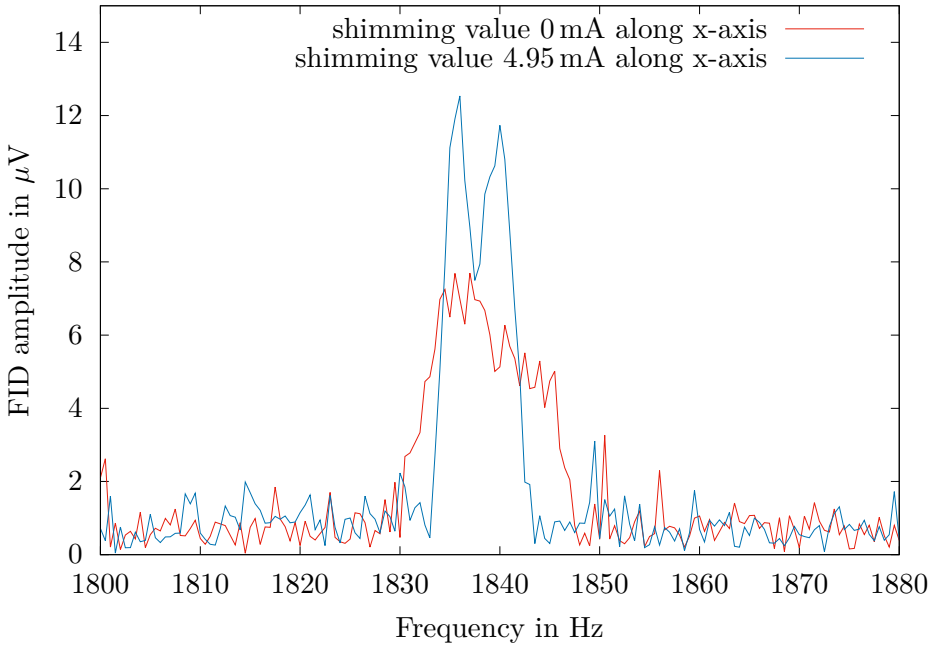


**Figure 3.13:** Spectrum of a single HAHN echo applied by different shimming values. Due to more de-shimming of the red curve, the amplitude is lower. Nevertheless the area under the spectrum is the same, due to the same magnetization.

For the following chapter it is specifically important to know which relaxation time we observe. Due to the inhomogeneous magnetic field there exist different relaxation times of the transversal relaxation time $T_2$. The transversal relaxation time $T_2^*$ describes the relaxation in consideration of the inhomogeneous magentic field. Therefore the formula

has the following shape:

$$\frac{1}{T_2^*} = \frac{1}{T_2} + \gamma \Delta B_0 \ . \tag{3.7}$$

In this equation $\gamma$ describes the gyromagnetic ratio of the probe and $\Delta B_0$ indicates the difference of the magnetic field to its equilibrium state. Therefore we know that every time we de-shim the system $T_2^*$ is observed and not $T_2$.

## 3.6 Multiple echo sequences

Besides one HAHN echo it is also possible to apply multiple HAHN echos in one experimental measurement. This method is called CALL-PURCELL-MEIBOOM-GILL-method (CPMG). Therefore the 180° pulse is applied every $2\tau$ and thus there occur many maxima in the signal every period of $2\tau$. The reason to use the CPMG method is that it is possible to measure the amplitude of two consecutive maxima more often and therefore the measurement of $T_2$ is more precise. This will be discussed in detail in the next chapter.
To make the CPMG signals smoother in the time domain we do not use rectangular functions for the pulses, but smoothen them at the edge by a *sine-bell-square* function. This is possible, due to the fact that it does not change the physical properties of our measurements, but will make them smoother.
A main advantage of CMPG is that errors in the refocusing pulse can be corrected (minimize term of inhomogeneous magnetic field), by changing the phase between the $B_1$ excitation and the refocusing pulses. The program *Prospa* provides a function called "Constant 180 pulse phase". This function keeps all the phases of the refocusing pulses equal. The second function *Prospa* provides is "Alternating 180 pulse phase". This function compensates echo errors by alternating the refocusing pulses by 180°. In figure 3.14 it is visible how a change in the 180 pulse phase affects the signal. Unfortunately we only saved the signal for 180 pulse phases of 270° and 90°. For those two values the signal does not change. That is also the reason why there is only one signal visible. The one depicted in blue colour lays just directly behind the red curve and is therefore not visible. If we would have saved a pulse phase of 0° or 180° the signal should change to a way faster decay and so the amplitude would fade away quickly.

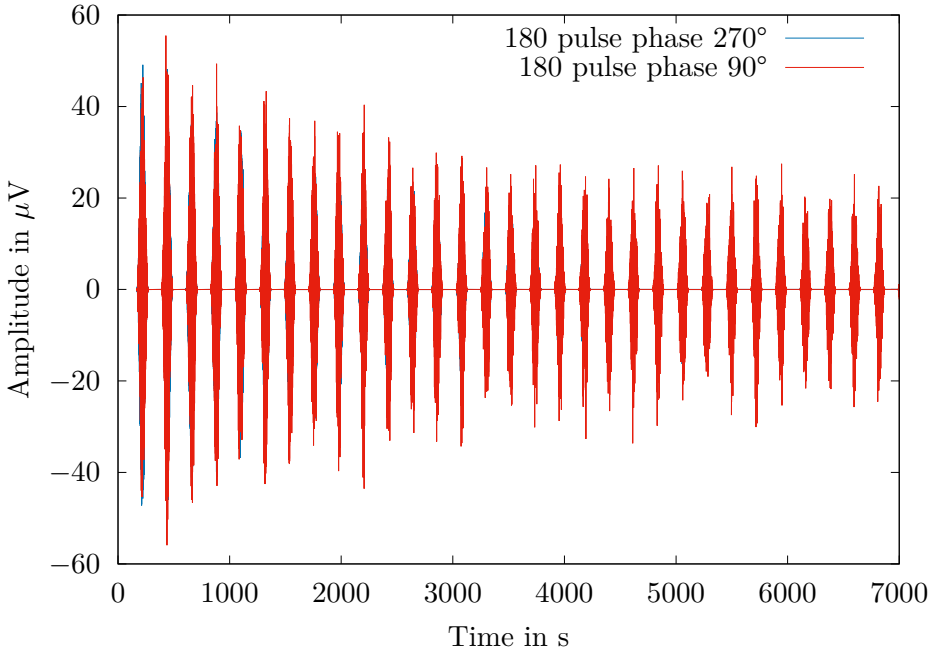


**Figure 3.14:** This figure shows the impact of the 180 pulse phase. Unfortunately we only saved data for a 180 pulse phase of 270° and 90° and for those values it is correct that the signal does not change, but a signal for a 180 pulse phase of 180° would have shown e.g. a faster decay of the signal.

## 3.7 Transversal relaxation measurements

The last chapter of the first part of this experiment concentrates on the transversal relaxation measurement. In order to do so there are two possible ways again.
The first one is by one single HAHN echo (spin echo). Therefore the ratio between the maximum of the signal after the 90° pulse and the maximum after the echo (maximum after $2\tau$) provides the transversal relaxation time $T_2$. Figure 3.15 shows measurements for this method by different echo time steps of $2 \cdot 400\,\text{ms}$. The exponential decay is clearly visible, due to the already explained loss of phase coherence between the spins. Therefore to fit the datapoints the following formula has been used:

$$M(x) = M_0 \cdot \exp\left(\frac{-x}{T_2}\right) \quad . \tag{3.8}$$

This formula shows a $T_2$ relaxation time of $2691(12)\,\text{ms}$. It is important to remember that the phase coherence loss because of the spin-spin relaxation is irreversible and is always obtained when measuring $T_2$.

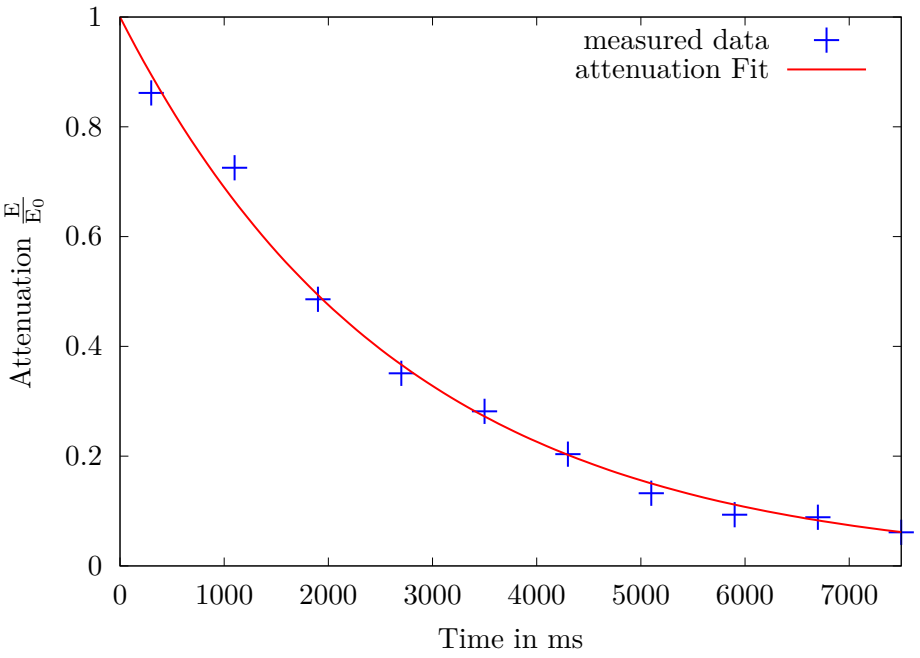


**Figure 3.15:** Attenuation $\frac{E}{E_0}$ for different echo times and exponential fit of the data. The applied exponential fit results in a value of $T_2 = 2691(12)$ ms.

One disadvantage of the $T_2$ measurement via one single HAHN echo is that the ratio of two back to back maxima is not that decisive. The second option to measure $T_2$ is by using CPMG. Now that more maxima can be observed, the ratio of back to back maxima can be calculated more precisely. Therefore the result of $T_2$ is more accurate using this method. Figure 3.16 shows measured data for 30 different echos. Due to the exponential decay formula (3.8) has been used again to fit the measured data. This results in a value for $T_2$ of 2317.760 00(62) ms. It is clearly visible that the uncertainty of this value is significantly lower than the value of the measurement via one single HAHN echo, therefore it is more exact. A comparison to an example literature value of 2000 ms [LLC] shows that the magnitude is correct. Keeping in mind that a comparison to literature values is just there to get the magnitude the result is satisfying. Since the surrounding magnetic field and the probe define the exact value as mentioned before.

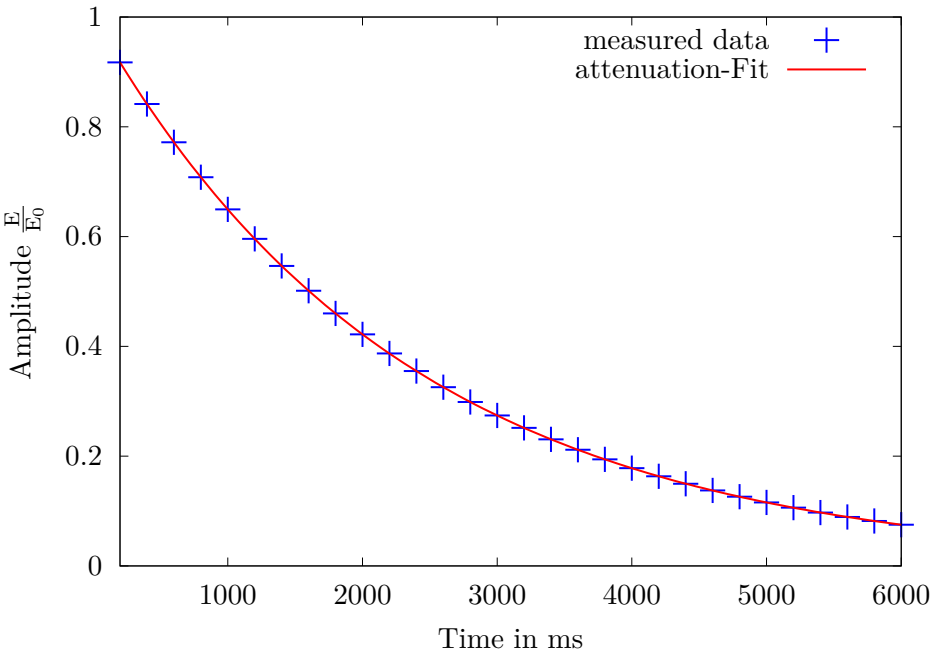


**Figure 3.16:** Attenuation $\frac{E}{E_0}$ for different echo maxima provided by the CPMG method. The applied exponential fit results in a value of $T_2 2317.760\,00(62)$ ms.

The difference of the two $T_2$ values might occur, due to de-shimming the system for the CPMG method and therefore some inaccurate pulse phases can have been measured. Nevertheless note that the CPMG method is the more precise method to measure $T_2$, due to more back to back maxima. By measuring $T_2$ via the HAHN echo and the CPMG the inhomogeneity of the magnetic field is reversed in theory, due to the 180° pulses. Therefore they should not have a big impact on the relaxation time. Nevertheless owing to inaccurate pulse phases, de-shimming can still have a small impact. That is probably the reason why the two measured relaxation times do not take on the same value.

# 4 Teil II – Anwendung

@Philipp ab hier Alle TITEL, BUs, LEGENDEN nochmal korrigieren!! ”todo”

## 4.1 ToDo!Fourietrafo der Messungen mit unterschieldicheer Polarisationszeit

Im zweiten Teil diese Berichts soll sich nun auf Anwendungsmöglichkeiten der Magnetresonanz Technologie im Erdmagnetfeld konzentriert werden.

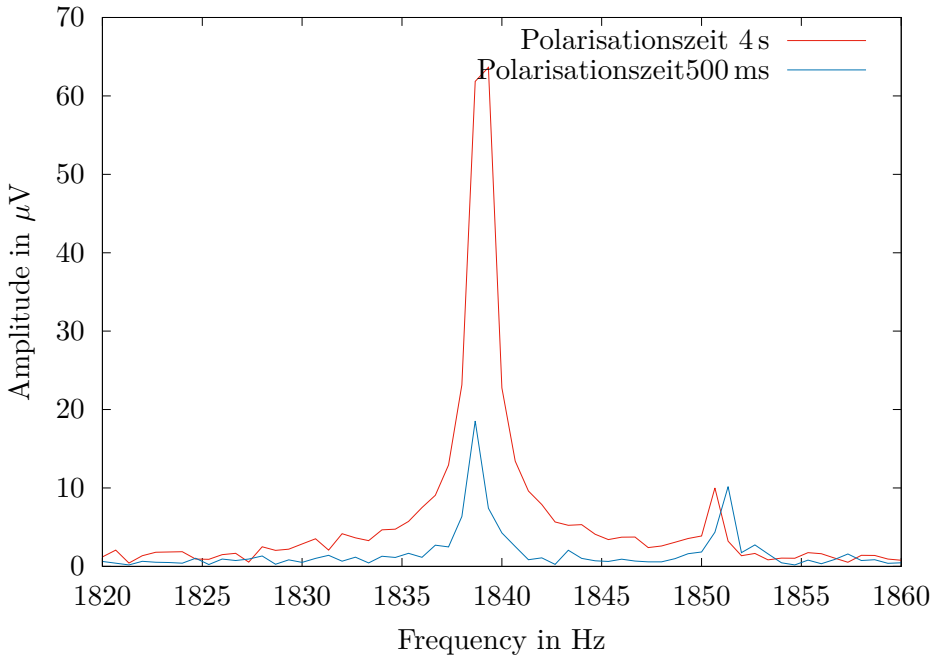


**Abbildung 4.1:** Amplitude in abhängigkeit von zwei verschiedenen Polarisatiosnzeiten

## 4.2 ToDo!T1 und T2 Relaxationszeit für Wasser und mit Zusatzmitteln

$Cu^{2+}$ $Mn^{2+}$

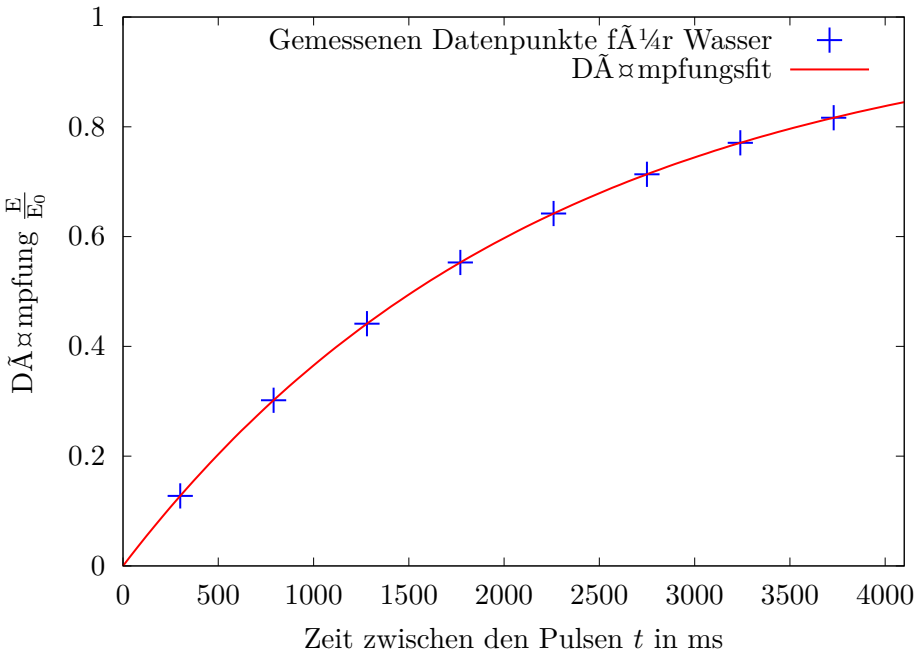


**Abbildung 4.2:** T1 Messung von Wasser

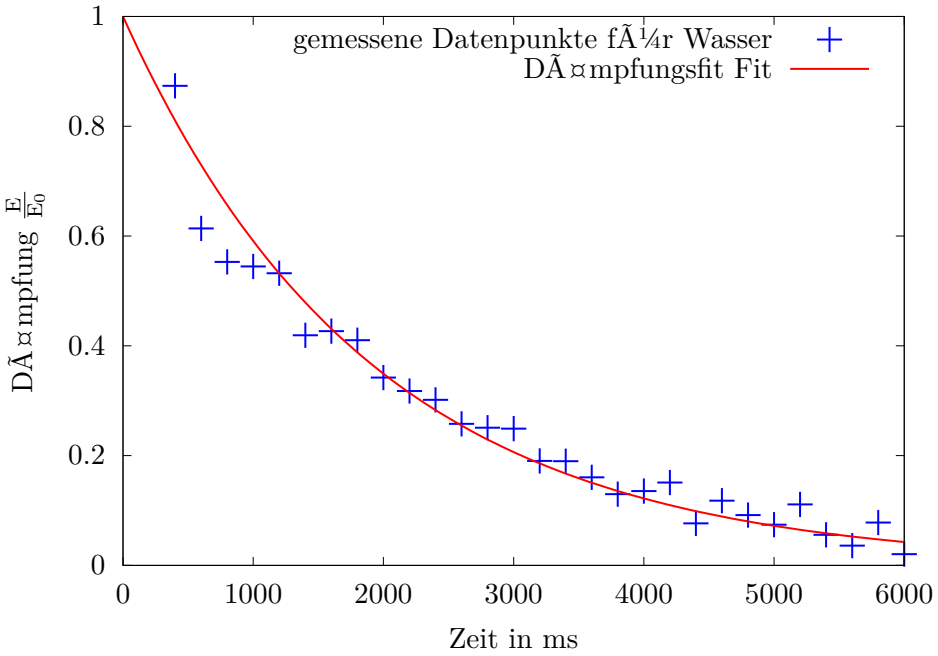


**Abbildung 4.3:** T2 Messung von Wasser

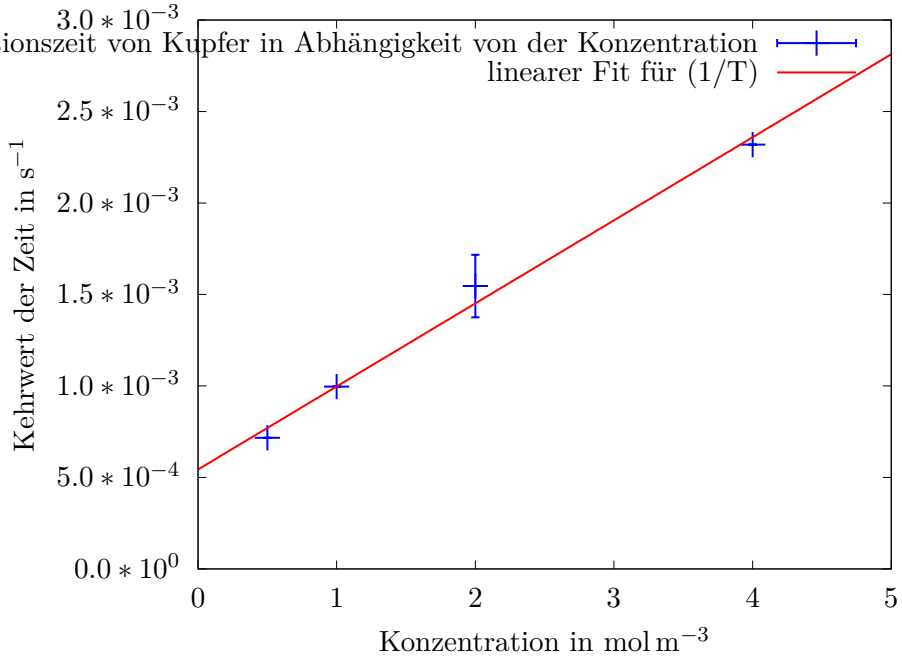


**Abbildung 4.4:** ToD:Relaxivitat $r_1$ von Kupfer

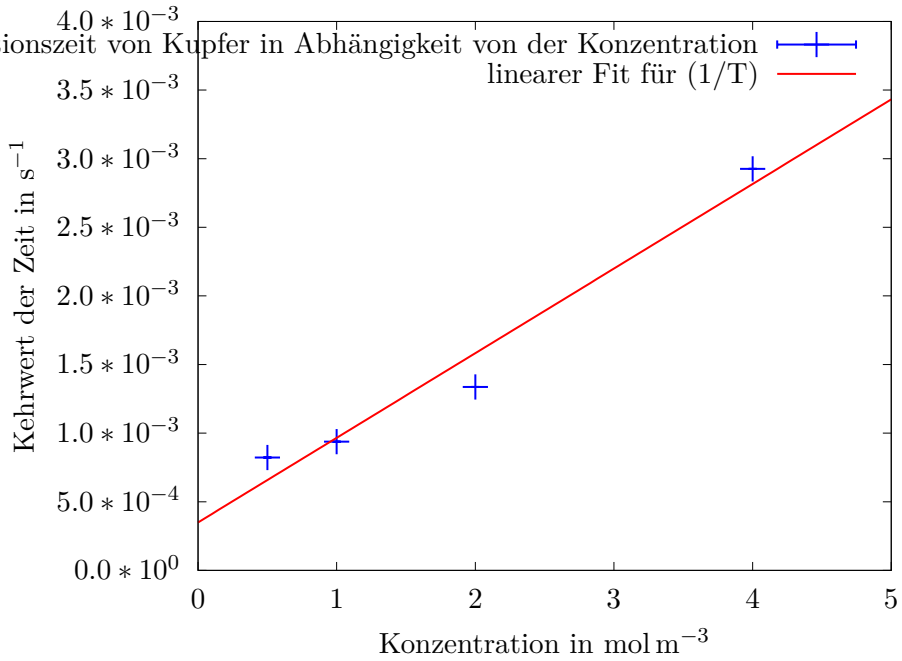


**Abbildung 4.5:** ToD:Relaxivitat $r_2$ von Kupfer

oke longitudinale Relaxationszeit von Mangan in Abhängigkeit von der Konzentration

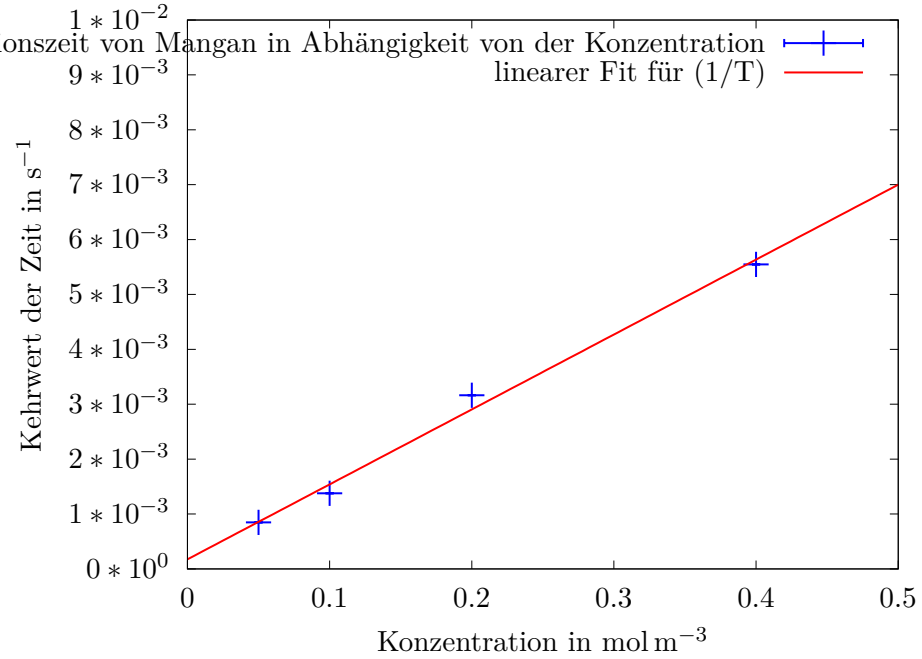


**Abbildung 4.6:** ToD:Relaxivitat $r_1$ von Mangan

roke transversale Relaxationszeit von Mangan in Abhängigkeit von der Konzentration

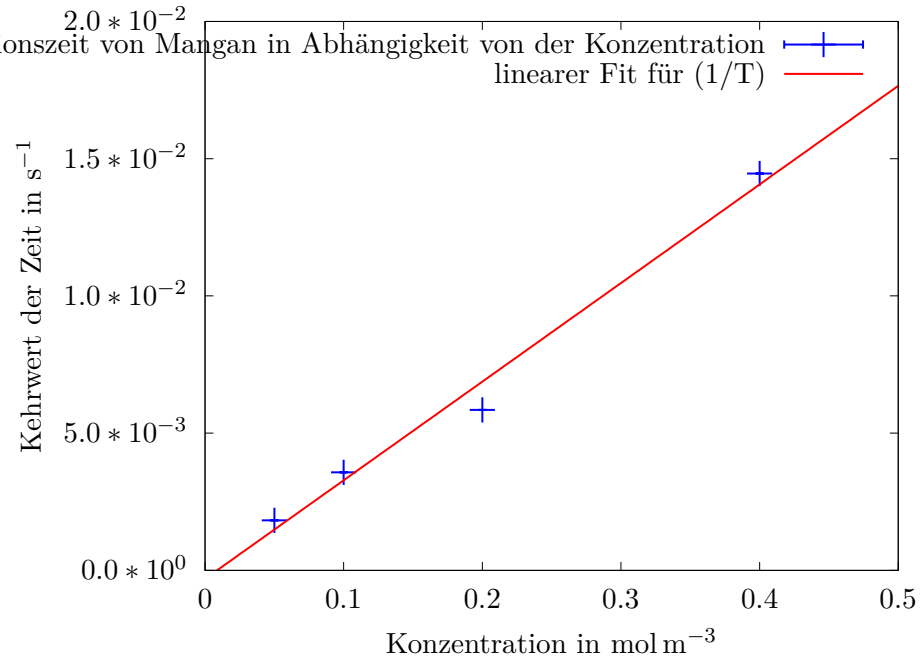


**Abbildung 4.7:** ToD:Relaxivitat $r_2$ von Mangan

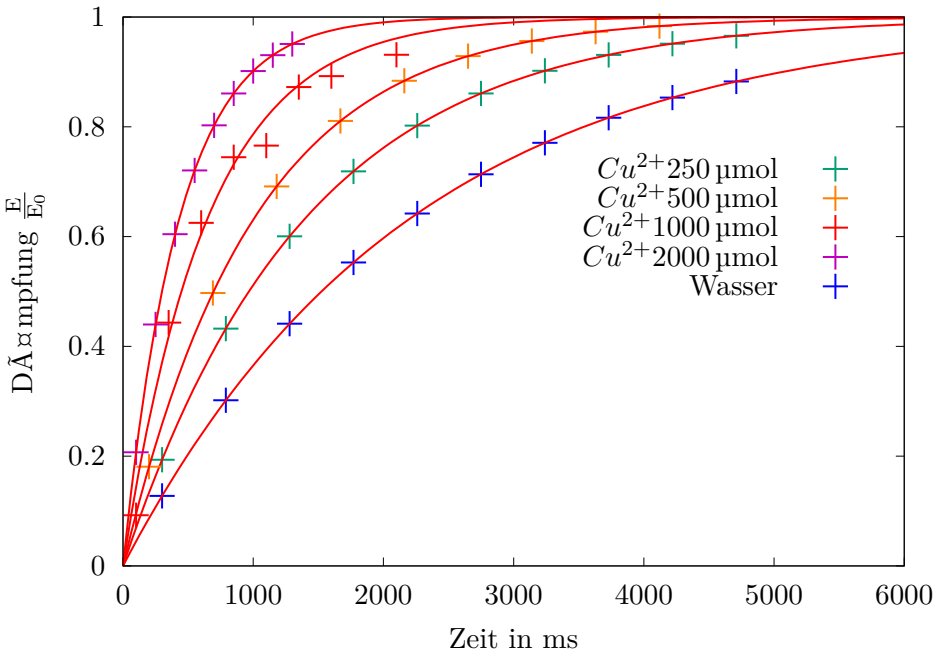


**Abbildung 4.8:** ToD:Alle Messungen T1 Cu2+

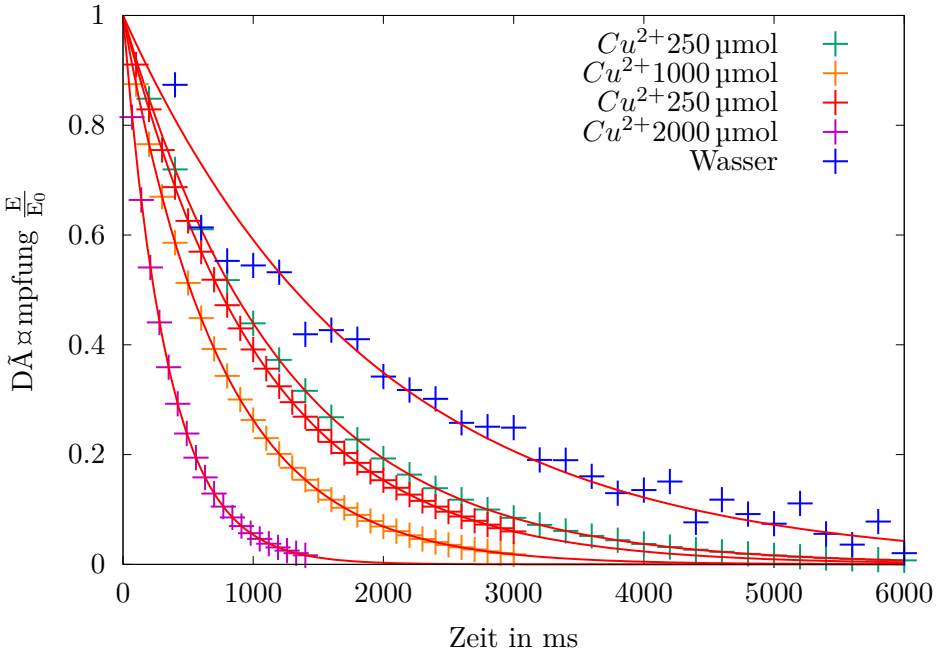


**Abbildung 4.9:** ToD:Alle Messungen T2Cu2+

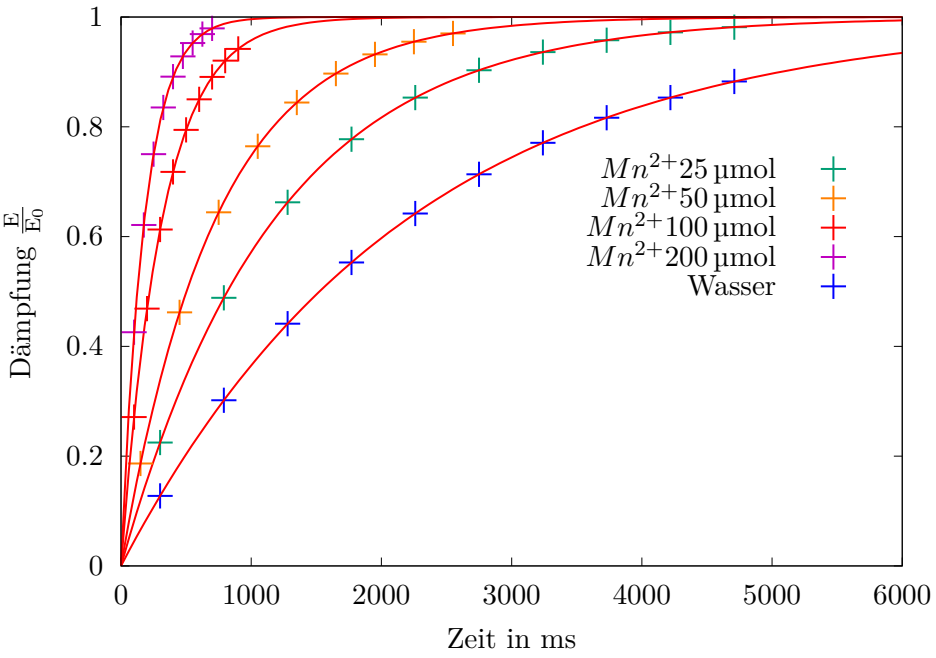


**Abbildung 4.10:** ToD:Alle Messungen T1Mn2+

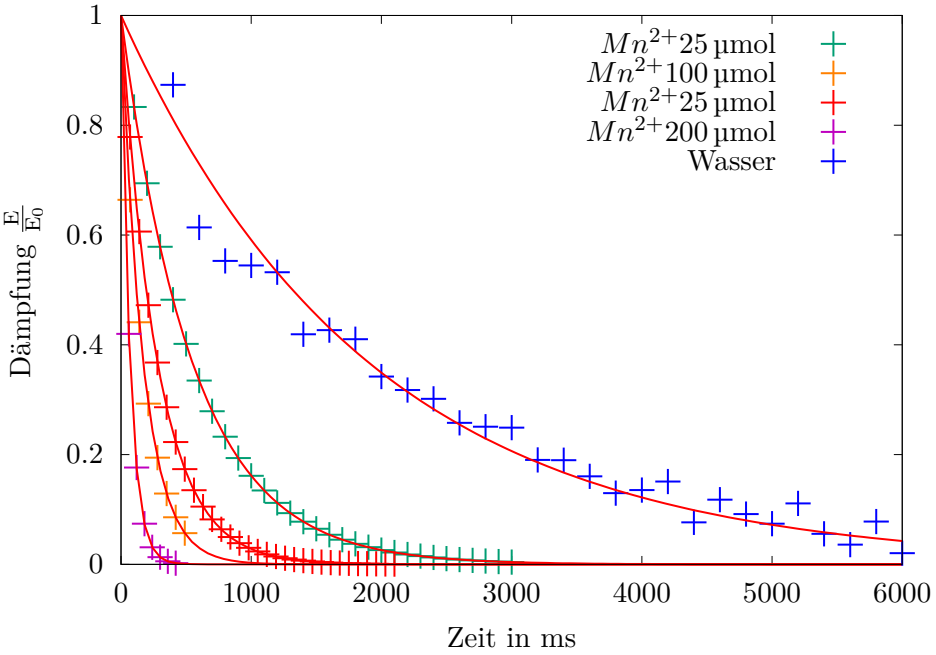


**Abbildung 4.11:** ToD:Alle Messungen T2MN2+

| | T1 | U(T1)-Fit | T2 | U(T2)-Fit |
|---|---|---|---|---|
| Cu2 250 | 1394,84 | 0,001055 | 1215,51 | 0,0002529 |
| Cu2 500 | 1003,4 | 0,0004851 | 1066,44 | 0,0002621 |
| Cu2 1000 | 646,849 | 71,54 | 748,404 | 0,0001937 |
| Cu2 2000 | 431,268 | 0,0002906 | 341,83 | 0,0001228 |

| | T1 | U(T1)-Fit | T2 | U(T2)-Fit |
|---|---|---|---|---|
| Wasser | 2199,46 | 0,003027 | 1901,06 | 89,83 |

| | T1 | U(T1)-Fit | T2 | U(T2)-Fit |
|---|---|---|---|---|
| Mn 2 25 | 1178,28 | 0,0009801 | 548,337 | 0,0001258 |
| Mn 2 50 | 725,857 | 0,0006027 | 279,858 | 0,00008179 |
| Mn 2 100 | 316,085 | 0,0003079 | 170,996 | 0,0001182 |
| Mn 2 200 | 180,244 | 0,0001274 | 69,1512 | 0,0000547 |

**Tabelle 4.1:** T1- und T2- abhängig von den Stoffen und der Konzentration

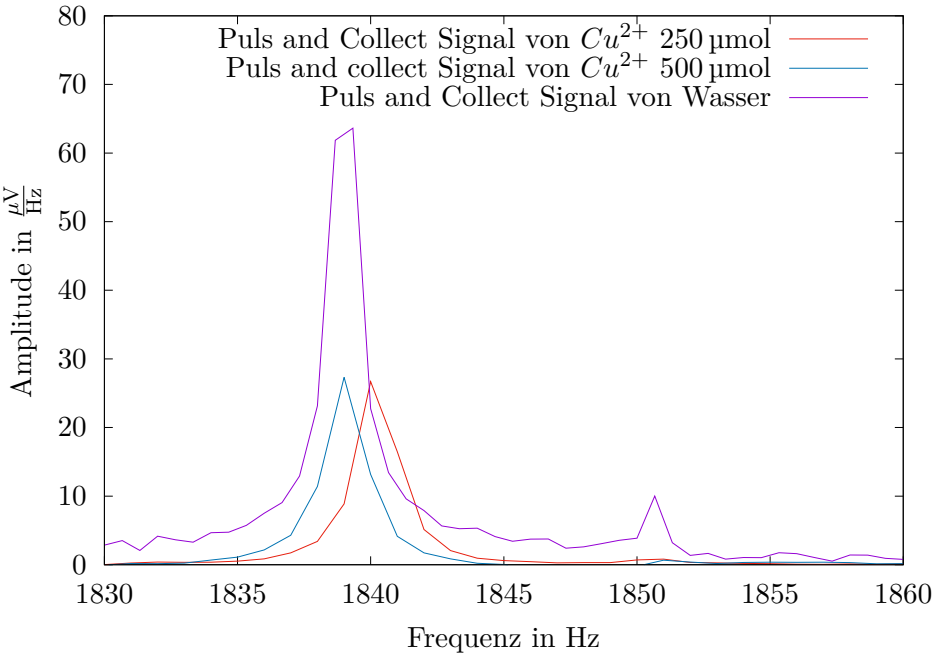


**Abbildung 4.12:** Die T1 Signale bei der jeweiligen Konzentration

**Tabelle 4.2:** Relaxivitäten von Kupfer und Mangan.

| | Kupfer | Mangan |
|---|---|---|
| $r_1$ in $\frac{\text{mol}}{\text{m}^3\text{s}}$ | $4.53(31) \cdot 10^{-4}$ | $1.365(84) \cdot 10^{-2}$ |
| $T_1$ in s | $1.84(24) \cdot 10^{3}$ | $5.7(63) \cdot 10^{3}$ |
| $r_2$ in $\frac{\text{mol}}{\text{m}^3\text{s}}$ | $6.16(84) \cdot 10^{-4}$ | $3.5930(31) \cdot 10^{-1}$ |
| $T_2$ in s | $2.9(16) \cdot 10^{3}$ | $-3.2(75) \cdot 10^{3}$ |

## 4.3 1D MRI

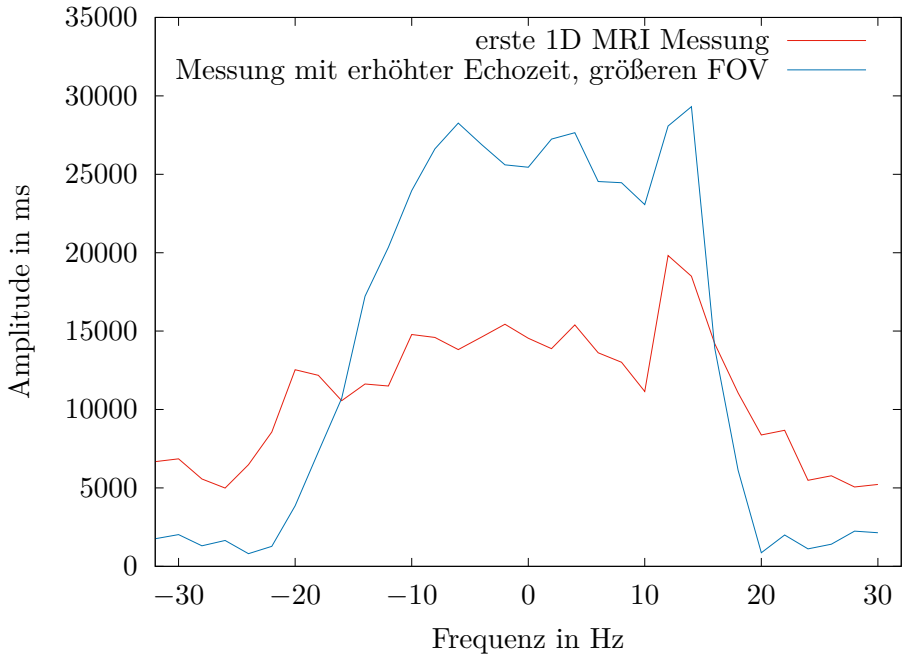


**Abbildung 4.13:** Anfangsmessung für verschiedene Echozeit und FOV

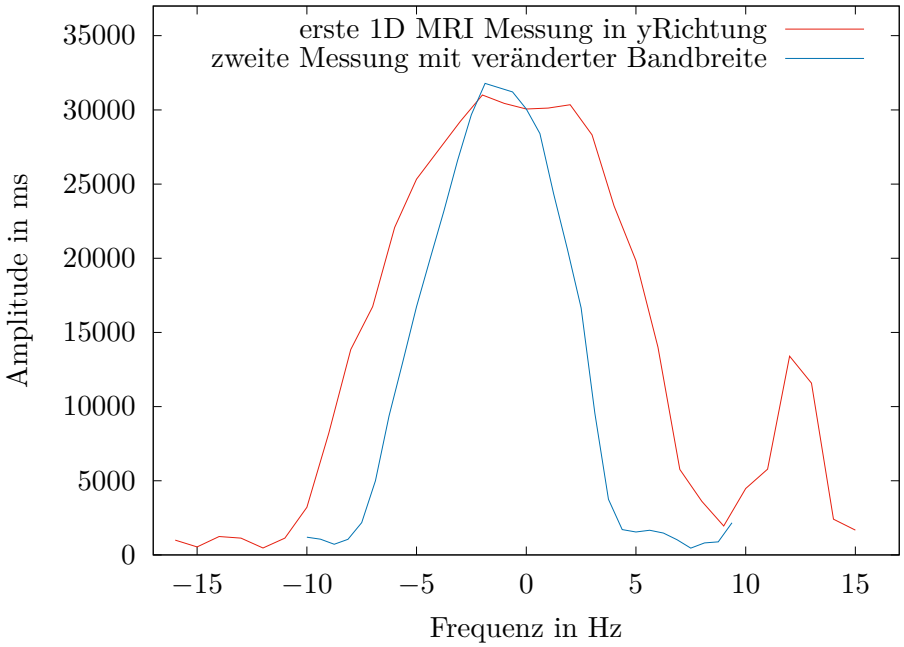


**Abbildung 4.14:** Messung vom 1D MRI in y-Richtung

## 4.4 2D MRI

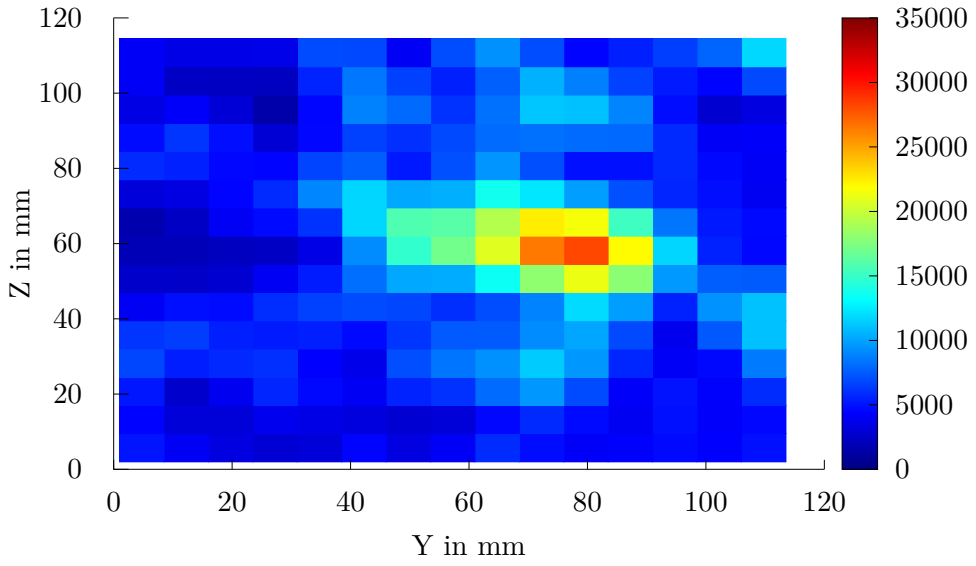


**Abbildung 4.15:** 2D MRI mit T1 600 ms

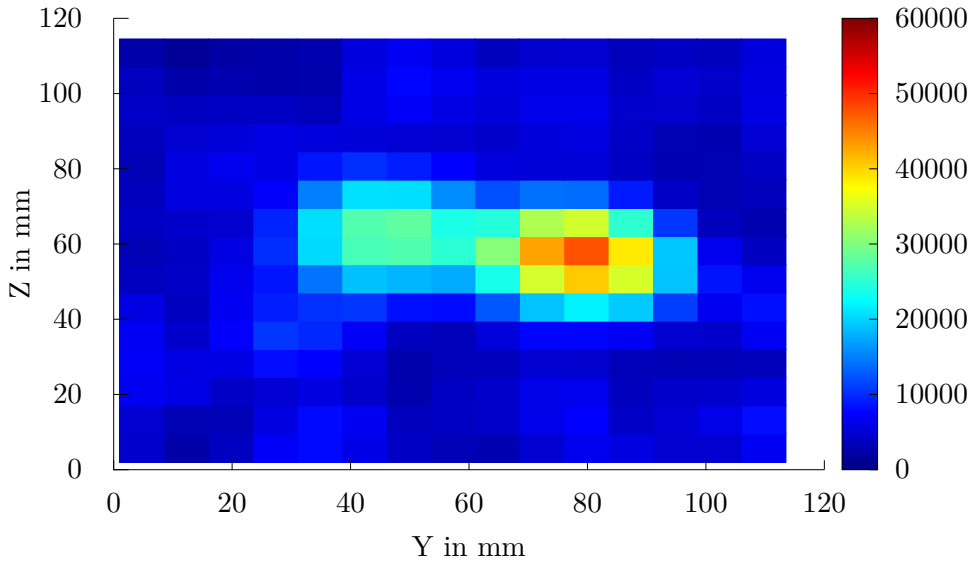


**Abbildung 4.16:** 2D MRI mit T1 1300 ms

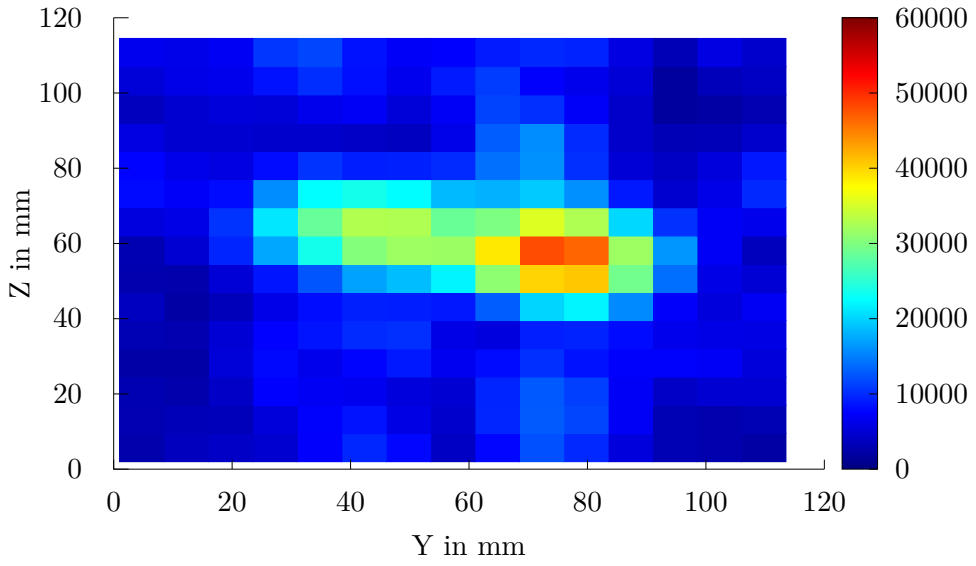


**Abbildung 4.17:** 2D MRI mit T1 2100 ms

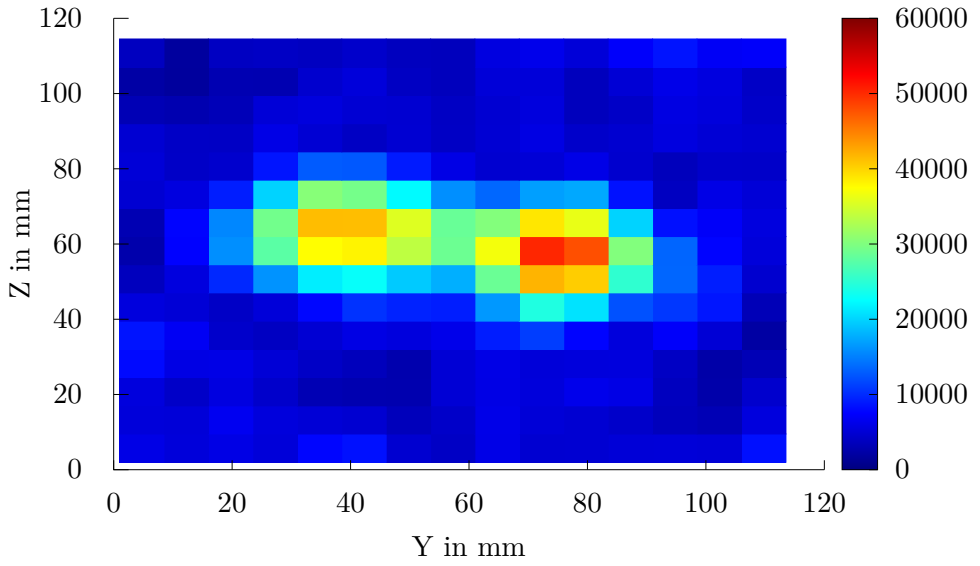


**Abbildung 4.18:** 2D MRI mit T1 2800 ms

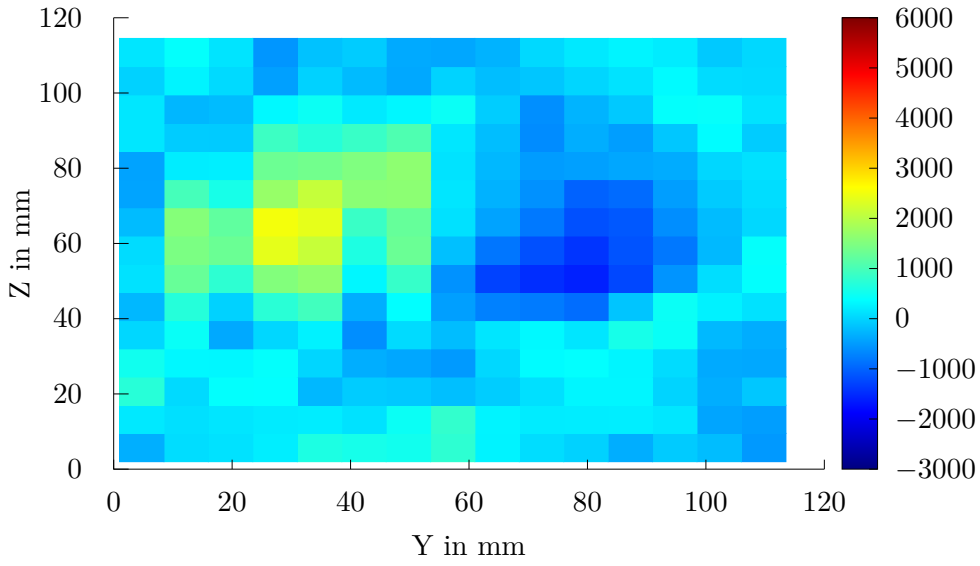


**Abbildung 4.19:** 2D MRI mit T2 200 ms

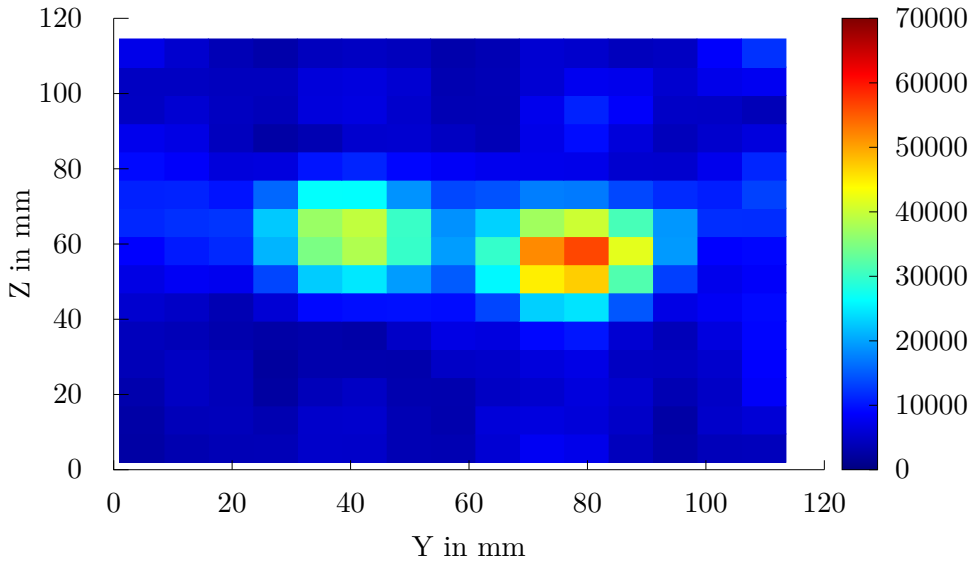


**Abbildung 4.20:** 2D MRI mit T2 250 ms

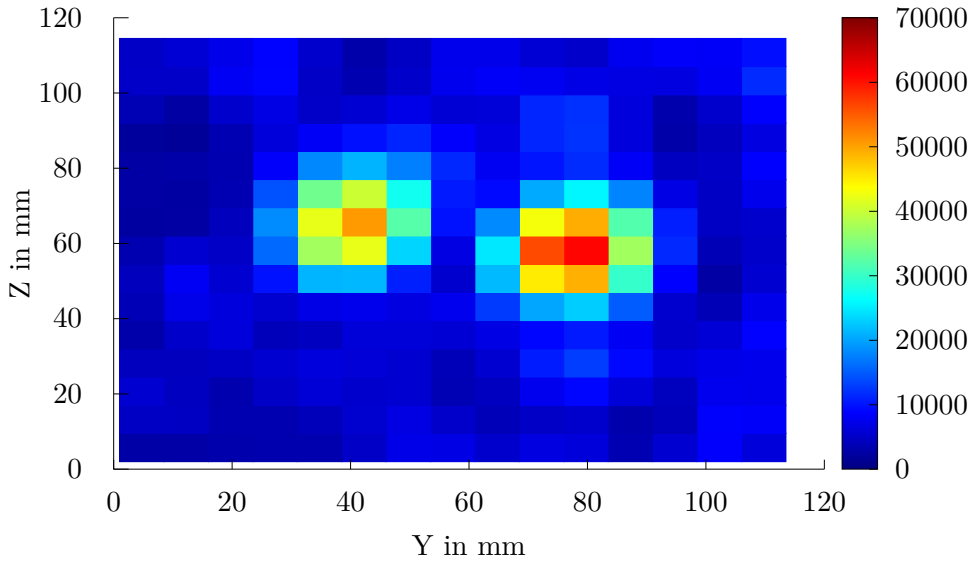


**Abbildung 4.21:** 2D MRI mit T2 300 ms

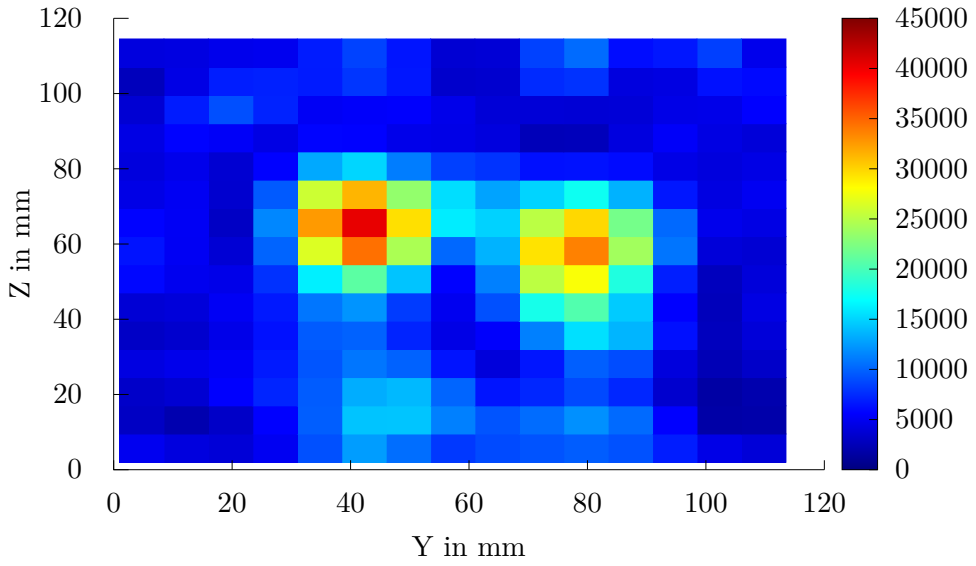


**Abbildung 4.22:** 2D MRI mit T2 450 ms

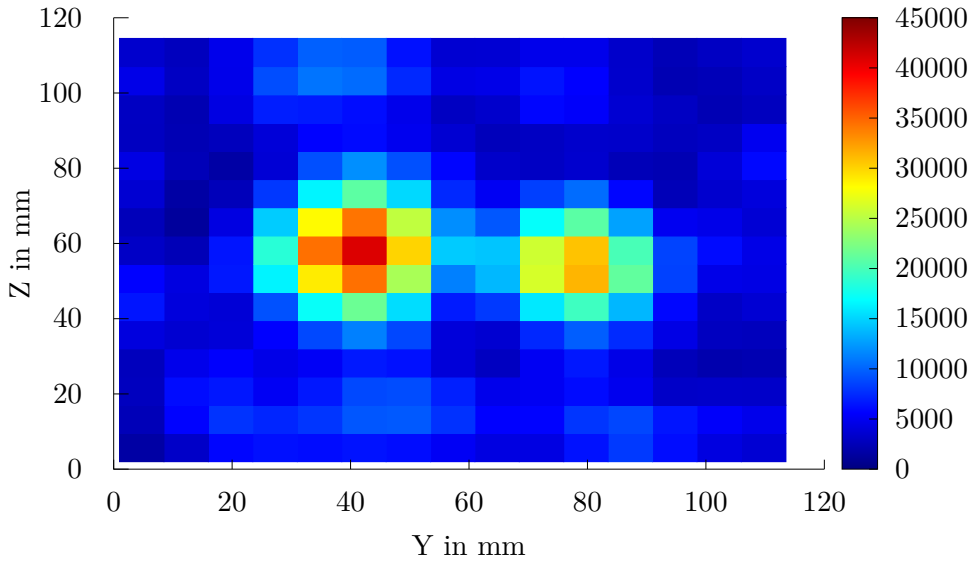


**Abbildung 4.23:** 2D MRI mit T2 550 ms

## 4.5 J-Kopplung zur chemischen Strukturanalyse

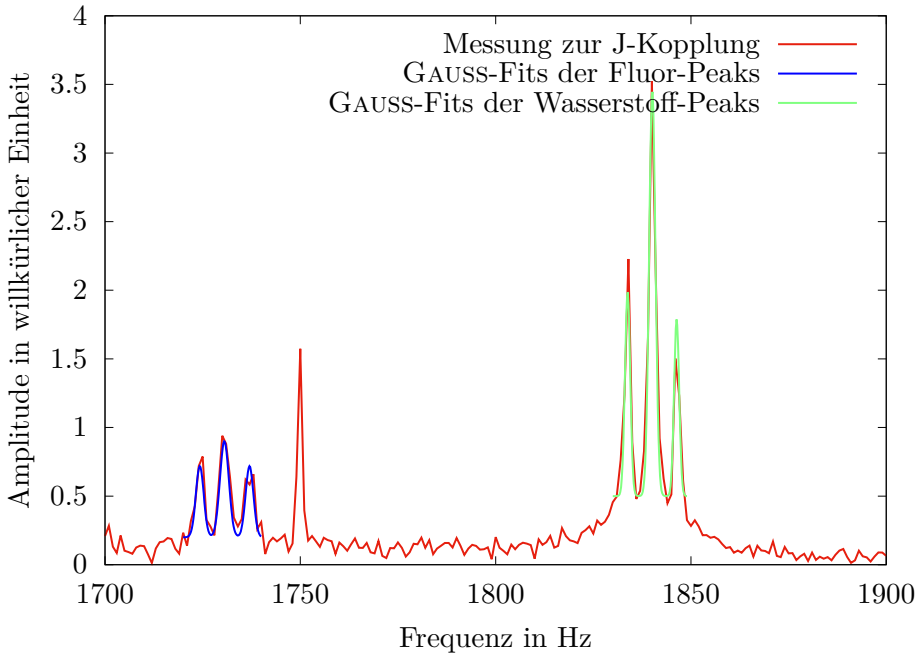


**Abbildung 4.24:** TODO!!;
Zum tunen benutzte Daten des Puls and collect Experiments; Man soll noch die Integrale berechnen der einzelnen Peaks(aus den Integralen bekommt man dann das Verhältnuis von 1:2:3:3:2:1 oder so halt); Diese Peaks fitten bzw den abstand der Maximas berechnen=< daraus dann die Kopplungaskostante

## 4.6 ToDo!T1 und T2 Relaxationszeit für Wasser und mit Zusatzmitteln

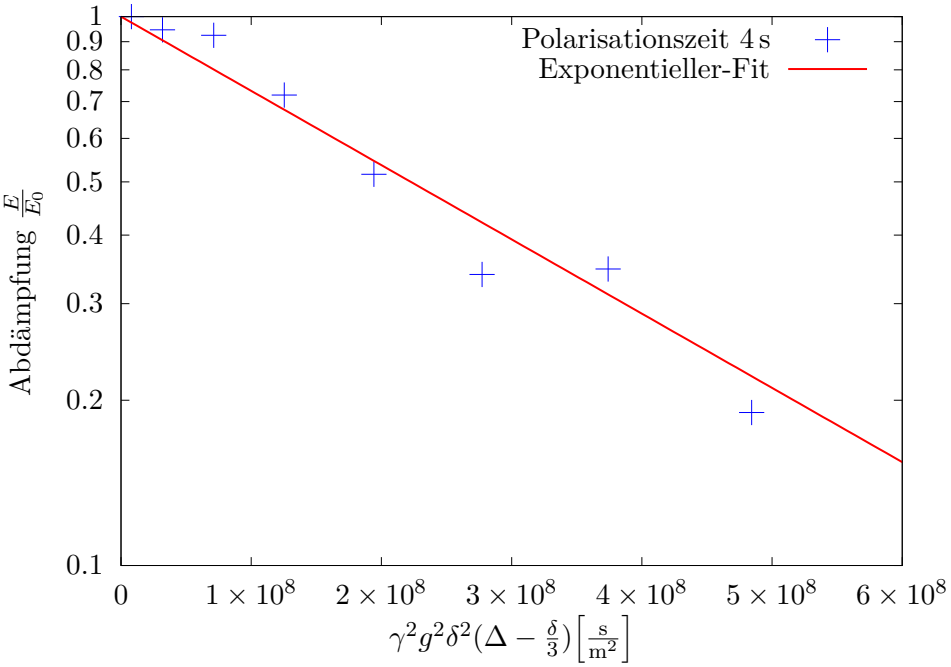


**Abbildung 4.25:** Diffusionskoeffizient $3.11 \cdot 10^{-9}\ \frac{\mathrm{m}^2}{\mathrm{s}}$

# 5 Error discussion and conclusion

Despite all measured data make sense and are consistent with the literature, there are also errors which occured. Lets begin by the setup and its position itself. Due to the orientation and position in the room the noise level in chapter 3.1 changes a lot. The noise level 7.5 $\mu$V is a value below 10 $\mu$V and therefore a acceptable noise level. To achieve excellent results it is even though necessary to have a noise level below 3 $\mu$V. Furthermore some of the measured data depend on the earths magnetic field and since this is not really strong (magnitude nT) even small metal objects can change its properties. The influence of the light source and the computer display were already discussed in the chapter 3.1. Even though the gradient coil should erase all inhomogeneous components of the magnetic field, there is always a slight propability that it is not homogeneous.
Another imperfection of the experiment is the duration of the pulses and the phases. With the help of figure 3.5 we analyzed that the $B_1$ duration for a 90° pulse is 1.35 ms. Since the measurement steps in the figure 3.5 are rather high, the duration could also change a little. This error has a huge impact when it comes to the *Hahn* echo and the CPMG method and thus changes $T_2$.
Despite all errors the results confirm the theorey and are consistent with the literature. This is allocable by the values for $T_{1,p}$ of 2912.8800(48) ms and for $T_{1,e}$ of 2753.0500(12) ms and for the measurements of $T_2$ of 2317.760 00(62) ms. The research of the hydrogen signal in a pulse and collect experiment results in a width of the peak at half maximum (FWHM) of 1.177(42) Hz and is therefore really small. With the help of those values, the discussion of the values and the detailed introduction, the experiment shows the properties of a basic ENMR experiment quite good.

## Literatur

[Adm] Administration, National: *Magnetic Field Calculators*. https://www.ngdc.noaa.gov/geomag/calculators/magcalc.shtml?#igrfgrid, looked up: 2020-07-21.

[LLC] LLC, Elster: *Size of T1 vs T2*. http://mri-q.com/why-is-t1--t2.html, looked up: 2020-07-21.

[Mor01] Mortazavi, Saideh Sadat: *Earth Field Magnetic Resonance Imaging And Paramagnetic Contrast Agents*, last update: 2009-01-01. https://scholarworks.utep.edu/cgi/viewcontent.cgi?article=3739&context=open_etd, looked up: 2020-07-16.

# Abbildungsverzeichnis